

TBA equations for the Schrödinger equation with a regular singularity

Katsushi Ito^a, Hongfei Shu^{b,a},

^a*Department of Physics, Tokyo Institute of Technology Tokyo, 152-8551, Japan,*

^b*Nordita, KTH Royal Institute of Technology and Stockholm University
Roslagstullsbacken 23, SE-106 91 Stockholm, Sweden*

Abstract

We derive the Thermodynamic Bethe Ansatz (TBA) equations for the Schrödinger equation with an arbitrary polynomial potential and a regular singular (simple and double pole) term. The TBA equations provide a non-trivial generalization of the ODE/IM correspondence and also give a solution for the Riemann-Hilbert problem in the exact WKB method. We study the TBA equations in detail for the linear and the harmonic oscillator potentials together with inverse and centrifugal terms. As an application, we also compute numerically the Voros spectrum for these potentials using the Bohr-Sommerfeld quantization condition.

1 Introduction

The exact WKB method for stationary one-dimensional Schrödinger equation has been studied extensively for many years [1–6]. The exact WKB periods (or the quantum periods) are asymptotic series in the Planck constant and therefore must be treated by Borel and lateral Laplace transformations. Resurgence helps us to understand the relation between perturbative and non-perturbative effects to the periods. In particular, their classical limit and discontinuity structure (the Stokes phenomena) determine the quantum periods completely. This analytic bootstrap program (or the Riemann-Hilbert problem) has been worked out for cubic and quartic potentials [3].

The Stokes phenomena for the solutions of the Schrödinger equation in the complex plane leads to the functional relations among the Wronskians of the solutions. Incorporating the basis of solutions around the origin, these functional relations are identified with the functional equations of the quantum integrable models such as T-Q relations, T-system and Y-system. This phenomena is known as the ODE/IM correspondence [7–10], which has been generalized to higher-order differential equations [11–18]. This relation has been studied mainly in the case of monic potential and the spectral problem has been solved by the NonLinear Integral Equations¹.

Similar Riemann-Hilbert problems also appear in the study of the BPS spectrum in $\mathcal{N} = 2$ supersymmetric gauge theories and the minimal surface in AdS background [26–38]. Inspired by these works, the discontinuity formula for a general polynomial potential has been reformulated in the form of the thermodynamic Bethe ansatz (TBA) equations [39], where exponential of the quantum periods over specific one-cycles are identified as the Y-functions and the Planck constant plays a role of the spectral parameter. From the wall-crossing of the TBA equations, one can study the quantum periods for a polynomial potential with generic complex coefficients. The TBA equations together with the exact quantization condition provide an efficient numerical method to solve the spectral problem of quantum mechanics.

An interesting generalization is to add inverse and centrifugal terms to the potential. For a monomial potential with a centrifugal term, the ODE/IM correspondence has been

¹See also [19–25] for the ODE/IM correspondence associated with affine Lie algebras.

studied in [7–10, 40]. The centrifugal term induces monodromy around the origin and the TBA system is extended to the D -type from the A -type. In this work, we will study the Y -system and the TBA equations for a general polynomial potential with a centrifugal potential. We will begin with the case where all the turning points are located along the real axis. It becomes a non-trivial problem to choose appropriate one-cycle on the WKB curve for the Y -functions since in the classical limit $\hbar \rightarrow 0$ some turning points degenerate and the next-order corrections to the WKB periods become divergent. In order to regularize classical turning points, we add an inverse potential. For the inverse potential, the structure of the WKB lines has been studied in [41–43]. We will show that there appear new Y -functions associated with non-trivial one-cycles on the Riemann surface and the TBA system is enhanced to the D -type. By applying the wall-crossing, we expect to relate the present TBA to the system in [7, 8]. But we will not discuss this issue in detail in this paper.

This paper is organized as follows. In section 2, we derive the Y -system from the Schrödinger equation with arbitrary polynomial potential incorporated with simple and double pole potentials. In section 3, we evaluate the asymptotic behavior of the Y -function and provide a closed TBA system. Some general properties of the TBA system are also presented. In section 4, we first re-derive the TBA equations from the discontinuity formula of WKB periods, which implies that our TBA equations govern the exact WKB periods. We then confirm numerically the TBA equations by comparing the expansion of the TBA equations at large θ and the higher-order corrections of WKB periods. As an application, we compute the Voros spectrum numerically using the Bohr-Sommerfeld quantization condition. Finally, we present conclusions and discussions in section 6. In appendix A, we derive the T - Q relation and the Bethe ansatz equation from the Schrödinger equation. In appendix B, some details of the wall crossing of the TBA equations are presented. In appendix C, we discuss the relations among the present ODE and other types of ODEs under a change of variable. This provides a further consistency check of the correspondence between the ODEs and the TBA systems.

2 Y-system from the Schrödinger-type equation

We consider the second order ODE of the Schrödinger type with a polynomial potential incorporated with a simple and a double pole terms:

$$\left(-\frac{d^2}{dz^2} + z^{r+1} + \sum_{a=1}^{r+2} b_a z^{r+1-a} + \frac{l(l+1)}{z^2} \right) \psi(z, b_a, l) = 0, \quad (1)$$

where z is a complex variable, r a non-negative integer, l a real parameter, and b_a , $a = 1, \dots, r+2$, complex parameters. This ODE possesses an irregular singularity at infinity and a regular singularity (simple and double pole) at origin. The double pole leads to a non-trivial monodromy around the origin, which is the main difference compared with the setup in [39].

We first consider the behavior of the solution around $z = \infty$. One finds the fastest decaying solution of (1) at infinity along the positive real axis behaves as [44]

$$y(z, b_a) \sim \frac{1}{\sqrt{2i}} z^{n_r} \exp\left(-\frac{2}{r+3} z^{\frac{r+3}{2}} \right), \quad (2)$$

where n_r are defined by

$$n_r = \begin{cases} -\frac{r+1}{4} & r : \text{even} \\ -\frac{r+1}{4} - B_{\frac{r+3}{2}} & r : \text{odd} \end{cases}. \quad (3)$$

B_m is defined by the following expansion:

$$\left(1 + \sum_{a=1}^{r+2} b_a z^{-a} + \frac{l(l+1)}{z^{r+3}} \right)^{1/2} =: 1 + \sum_{m=1}^{\infty} B_m z^{-m}. \quad (4)$$

The equation (1) is invariant under the Symanzik rotation $(z, b_a, l) \rightarrow (\omega z, \omega^a b_a, l)$:

$$\omega^{-2} \left(-\frac{d^2}{dz^2} + \omega^{r+3} z^{r+1} + \omega^{r+3} \sum_{a=1}^{r+2} b_a z^{r+1-a} + \frac{l(l+1)}{z^2} \right) \psi(\omega z, \omega^a b_a, l) = 0 \quad (5)$$

with $\omega = e^{\frac{2\pi i}{r+3}}$. By using the Symanzik rotation, we can construct a new solution y_k ($k \in \mathbb{Z}$) from y :

$$y_k(z, b_a, l) = \omega^{\frac{k}{2}} y(\omega^{-k} z, \omega^{-ak} b_a, l). \quad (6)$$

Since l does not change under the Symanzik rotation, we will omit the argument l in the solution. The solution y_k is subdominant in the sector \mathcal{S}_k , which is defined by

$$\mathcal{S}_k = \left\{ z \in \mathbb{C} : \left| \arg(z) - \frac{2k\pi}{r+3} \right| < \frac{\pi}{r+3} \right\}. \quad (7)$$

But $y_{k\pm 1}$ is a dominant solution in the sector \mathcal{S}_k . Then we can choose $\{y_k, y_{k+1}\}$ as a basis of the solutions of (1). We define the Wronskian of y_{k_1} and y_{k_2} by

$$W_{k_1, k_2}(b_a) \equiv W[y_{k_1}(z, b_a), y_{k_2}(z, b_a)] = y_{k_1}(z, b_a) \partial_z y_{k_2}(z, b_a) - y_{k_2}(z, b_a) \partial_z y_{k_1}(z, b_a). \quad (8)$$

One finds $W_{k_1, k_2}^{[2]}(b_a) = W_{k_1+1, k_2+1}(b_a)$, where we have introduced the j -shift of the phase in the arguments of a function by

$$f^{[j]}(z, b_a) := f(\omega^{-j/2} z, \omega^{-ja/2} b_a) \quad (9)$$

for an integer j . In our normalization (2), the Wronskian of y_k and y_{k+1} is evaluated as

$$W_{k, k+1}(b_a) = \begin{cases} 1 & r : \text{even} \\ \omega^{(-1)^k B \frac{r+3}{2}} & r : \text{odd} \end{cases}. \quad (10)$$

When we choose $\{y_0, y_1\}$ as the basis, y_k is expanded as

$$y_k(x, b_a) = \frac{W_{k,1}}{W_{0,1}} y_0(x, b_a) + \frac{W_{0,k}}{W_{0,1}} y_1(x, b_a). \quad (11)$$

2.1 Monodromy around origin

Next, we consider the monodromy of the solutions around the origin. Note that the sectors \mathcal{S}_k provide a multi-cover for the complex plane, where consecutive $r+3$ sectors cover the single complex plane. Since $y_{j+r+3}(z)$ and $y_j(z e^{-2\pi i})$ are the decaying solutions at infinity in the same sector, $y_{j+r+3}(z) \propto y_j(z e^{-2\pi i})$. From the definition (6), we find

$$y_{r+3}(z, b_a) = \omega^{\frac{r+3}{2}} y_0(e^{-2\pi i} z, b_a). \quad (12)$$

By acting the Symanzik rotation on both sides, one finds

$$y_{r+4}(z, b_a) = \omega^{\frac{r+3}{2}} y_1(e^{-2\pi i} z, b_a). \quad (13)$$

Since y_{r+3} and y_{r+4} are expanded in the basis $\{y_0, y_1\}$, $y_0(e^{-2\pi i} z)$ and $y_1(e^{-2\pi i} z)$ are also expanded in the same basis. Let us introduce the monodromy matrix $\Omega(b_a, l)$ by

$$\begin{pmatrix} y_1 \\ y_0 \end{pmatrix} (e^{-2\pi i} z) = \Omega(b_a, l) \begin{pmatrix} y_1 \\ y_0 \end{pmatrix} (z). \quad (14)$$

Then the relations (12) and (13) imply

$$\begin{pmatrix} y_{r+4} \\ y_{r+3} \end{pmatrix} (z) = \omega^{\frac{r+3}{2}} \Omega(b_a, l) \begin{pmatrix} y_1 \\ y_0 \end{pmatrix} (z). \quad (15)$$

From (11), one finds the monodromy matrix $\Omega(b_a, l)$ can be expressed in terms of the Wronskians:

$$\Omega(b_a, l) = \omega^{-\frac{r+3}{2}} \begin{pmatrix} \frac{W_{0,r+4}}{W_{0,1}} & \frac{W_{r+4,1}}{W_{0,1}} \\ \frac{W_{0,r+3}}{W_{0,1}} & \frac{W_{r+3,1}}{W_{0,1}} \end{pmatrix}, \quad (16)$$

whose trace is evaluated as

$$\text{Tr}[\Omega(b_a, l)] = \omega^{-\frac{r+3}{2}} \left(\frac{W_{0,r+4}}{W_{r+3,r+4}} + \frac{W_{r+3,1}}{W_{0,1}} \right). \quad (17)$$

From the power series solutions of the Schrödinger-type equation (1) around the origin, we can evaluate the trace of monodromy matrix. In the small z region, there are power series solutions of the form

$$\psi_+(z, b_a, l) = z^{l+1} + \mathcal{O}(z^{l+3}), \quad \psi_-(z, b_a, l) = z^{-l} + \mathcal{O}(z^{-l+2}). \quad (18)$$

$\{\psi_+, \psi_-\}$ forms a basis of the solutions around $z = 0$. The monodromy matrix $\mathcal{M}(b_a, l)$ for the basis (ψ_+, ψ_-) is defined by

$$\begin{pmatrix} \psi_+ \\ \psi_- \end{pmatrix} (e^{-2\pi i} z, b_a) = \mathcal{M}(b_a, l) \begin{pmatrix} \psi_+ \\ \psi_- \end{pmatrix} (z), \quad \mathcal{M}(b_a, l) = \begin{pmatrix} e^{-2\pi(l+1)i} & 0 \\ 0 & e^{2\pi li} \end{pmatrix}, \quad (19)$$

which is diagonalized in this basis. Their Wronskian of ψ_+ and ψ_- is evaluated as

$$W[\psi_+, \psi_-] = -(2l + 1). \quad (20)$$

In terms of the new basis $\{\psi_+, \psi_-\}$, y_0 and y_1 can be expanded as

$$\begin{pmatrix} y_1 \\ y_0 \end{pmatrix} (z) = \mathcal{Q}(b_a) \begin{pmatrix} \psi_+ \\ \psi_- \end{pmatrix} (z). \quad (21)$$

The matrix $\mathcal{Q}(b_a)$ defines the Q-functions of certain integrable models. The functional relations satisfied by $\mathcal{Q}(b_a)$ can be found in the appendix A. The monodromy matrix $\Omega(b_a, l)$ is diagonalized by $\mathcal{Q}(b_a, l)$ as

$$\Omega(b_a, l) = \mathcal{Q}(b_a) \mathcal{M} \mathcal{Q}(b_a)^{-1}. \quad (22)$$

Then the trace of the monodromy matrix is given by

$$\text{Tr}[\Omega(b_a, l)] = \text{Tr}[\mathcal{M}(b_a, l)] = 2 \cos(2\pi l), \quad (23)$$

which depends only on l .

2.2 Truncated Y-system

From the Q-functions $\mathcal{Q}(b_a)$, we can derive the Baxter's T-Q relations and the Bethe ansatz equations, which are explained in Appendix A. In this subsection, we focus on the Y-system. Following the construction in [39], we introduce the Y-functions

$$\begin{aligned}\mathcal{Y}_{2j}(b_a) &:= \frac{W_{-j,j}W_{-j-1,j+1}}{W_{-j-1,-j}W_{j,j+1}}(b_a), \\ \mathcal{Y}_{2j+1}(b_a) &= \left[\frac{W_{-j-1,j}W_{-j-2,j+1}}{W_{-j-2,-j-1}W_{j,j+1}}(b_a) \right]^{[+1]}, \quad j \in \mathbb{Z}_{\geq 0}.\end{aligned}\tag{24}$$

These can be written as

$$\mathcal{Y}_s(b_a) = \left[\frac{W_{0,s}W_{-1,s+1}}{W_{-1,0}W_{s,s+1}}(b_a) \right]^{[-s]}, \quad s = 0, 1, 2, \dots\tag{25}$$

Note that $\mathcal{Y}_0(b_a) = 0$ by definition. By using the Plücker relation for the 2×2 matrices:

$$W_{k_1+1,k_2+1}W_{k_1,k_2} = -W_{k_1+1,k_2}W_{k_2+1,k_1} - W_{k_1+1,k_1}W_{k_2,k_2+1},\tag{26}$$

we find the Y-functions (25) satisfy the relations

$$\mathcal{Y}_s^{[+1]}(b_a)\mathcal{Y}_s^{[-1]}(b_a) = \left(1 + \mathcal{Y}_{s-1}(b_a)\right)\left(1 + \mathcal{Y}_{s+1}(b_a)\right), \quad s = 0, 1, 2, \dots\tag{27}$$

This defines the A-type Y-system. Let us consider the Y-function \mathcal{Y}_{r+2} . From the definition (25), $(r+2)$ -shift of \mathcal{Y}_{r+2} is given by

$$\mathcal{Y}_{r+2}^{[r+2]}(b_a) = \frac{W_{0,r+2}W_{-1,r+3}}{W_{-1,0}W_{r+2,r+3}}(b_a).\tag{28}$$

By using the trace formula of monodromy matrix (17), we find

$$\frac{W_{-1,r+3}}{W_{r+2,r+3}}(b_a) = \omega^{\frac{r+3}{2}} \text{Tr}[\Omega(b_a, l)]^{[-2]} + \frac{W_{0,r+2}}{W_{r+2,r+3}}(b_a).\tag{29}$$

Substituting this into (28), we get

$$\mathcal{Y}_{r+2}^{[r+2]}(b_a) = \omega^{\frac{r+3}{2}} \hat{\mathcal{Y}}^{[r+2]} \text{Tr}[\Omega(b_a, l)]^{[-2]} + \left(\hat{\mathcal{Y}}^{[r+2]}(b_a)\right)^2,\tag{30}$$

where we have introduced a new Y-function $\hat{\mathcal{Y}}(b_a)$ by

$$\hat{\mathcal{Y}}(b_a) = \left[\frac{W_{0,r+2}}{W_{-1,0}}(b_a) \right]^{[-(r+2)]}.\tag{31}$$

and used $W_{-1,0} = W_{r+2,r+3}$. The functional relation for \mathcal{Y}_{r+1} thus becomes

$$\mathcal{Y}_{r+1}^{[+1]}(b_a)\mathcal{Y}_{r+1}^{[-1]}(b_a) = \left(1 + \mathcal{Y}_r(b_a)\right)\left(1 + \omega^{\frac{r+3}{2}}\text{Tr}[\Omega(b_a, l)]^{[-r-4]}\hat{\mathcal{Y}}(b_a) + \hat{\mathcal{Y}}(b_a)^2\right). \quad (32)$$

Moreover, by using the Plücker relation we find the relation for $\hat{\mathcal{Y}}$. In summary, we obtain a closed Y-system

$$\begin{aligned} \mathcal{Y}_s^{[+1]}(b_a)\mathcal{Y}_s^{[-1]}(b_a) &= \left(1 + \mathcal{Y}_{s-1}(b_a)\right)\left(1 + \mathcal{Y}_{s+2}(b_a)\right), \quad s = 1, \dots, r, \\ \mathcal{Y}_{r+1}^{[+1]}(b_a)\mathcal{Y}_{r+1}^{[-1]}(b_a) &= \left(1 + \mathcal{Y}_r(b_a)\right)\left(1 + \omega^{\frac{r+3}{2}}e^{2\pi il}\hat{\mathcal{Y}}(b_a)\right)\left(1 + \omega^{\frac{r+3}{2}}e^{-2\pi il}\hat{\mathcal{Y}}(b_a)\right), \\ \hat{\mathcal{Y}}^{[+1]}(b_a)\hat{\mathcal{Y}}^{[-1]}(b_a) &= 1 + \mathcal{Y}_{r+1}(b_a), \end{aligned} \quad (33)$$

where we used the trace of monodromy (23). Note that this is a D_{r+3} type Y-system. To derive the TBA equations from this Y-system, one needs to consider the functions with different values of b_a at the same time, which is very complicated in general. To solve this problem, we will follow the procedure in [39] where we introduce the spectral parameter ζ in the ODE (1).

2.3 New Y-system

Let us introduce the spectral parameter ζ , and rescale the variables in (1) as

$$x = \zeta^{\frac{2}{r+3}}z, \quad u_a = \zeta^{\frac{2a}{r+3}}b_a, \quad a = 1, 2, \dots, r+2. \quad (34)$$

In terms of the new variables, the equation (1) can be written in the form of the Schrödinger equation:

$$\left(-\zeta^2 \frac{d^2}{dx^2} + x^{r+1} + \sum_{a=1}^{r+2} u_a x^{r+1-a} + \frac{\zeta^2 l(l+1)}{x^2}\right)\hat{\psi}(x, u_a, \zeta) = 0, \quad (35)$$

where the spectral parameter ζ plays the role of \hbar and the potential is given by

$$V(x) = Q_0(x) + \zeta^2 Q_2(x), \quad (36)$$

$$Q_0(x) = \sum_{a=1}^{r+2} u_a x^{r+1-a}, \quad Q_2(x) = \frac{l(l+1)}{x^2}, \quad (37)$$

where the second term $\zeta^2 Q_2(x)$ represents the centrifugal potential. We can then regard the solution $y(z, b_a)$ as the function of ζ , x and u_a :

$$\hat{y}(x, u_a, \zeta) = y(z, b_a) = y\left(\zeta^{-\frac{2}{r+2}}x, -\zeta^{-\frac{2(a+1)}{r+3}}u_a\right), \quad a = 1, \dots, r+2. \quad (38)$$

The action of the Symanzik rotation $(z, b_a, l) \rightarrow (\omega^{-k}z, \omega^{-ka}b_a, l)$ can be expressed by the shift of the phase of ζ :

$$(\omega^{-k}z, \omega^{-ka}b_a, l) = \left((e^{i\pi k}\zeta)^{-\frac{2}{r+3}}x, (e^{i\pi k}\zeta)^{-\frac{2a}{r+3}}u_a, l \right), \quad a = 1, \dots, r+2. \quad (39)$$

The solutions $y_k(z, b_a)$ thus can be obtained from $\hat{y}(x, u_a, \zeta)$ by using

$$\hat{y}_k(x, u_a, \zeta) = \omega^{\frac{k}{2}}\hat{y}(x, u_a, e^{i\pi k}\zeta). \quad (40)$$

We also introduce the Wronskian of \hat{y}_j by

$$\hat{W}_{k_1, k_2}(\zeta, u_a) = \zeta^{\frac{2}{r+3}} \left(\hat{y}_{k_1}(x, u_a, \zeta) \partial_x \hat{y}_{k_2}(x, u_a, \zeta) - \hat{y}_{k_2}(x, u_a, \zeta) \partial_x \hat{y}_{k_1}(x, u_a, \zeta) \right). \quad (41)$$

This is normalized such that it agrees with $W_{k_1, k_2}(b_a)$. Using the Wronskians, we redefine the Y-functions $\mathcal{Y}_s(b_a)$ and $\hat{\mathcal{Y}}(b_a)$ as the functions of ζ and u_a , which are denoted as $Y_s(\zeta, u_a)$ and $\hat{Y}(\zeta, u_a)$, respectively. Explicitly they are defined by

$$\begin{aligned} Y_{2j}(\zeta, u_a) &= \frac{\hat{W}_{-j, j} \hat{W}_{-j-1, j+1}}{\hat{W}_{-j-1, -j} \hat{W}_{j, j+1}}(\zeta, u_a), \\ Y_{2j+1}(e^{-\frac{\pi i}{2}}\zeta, u_a) &= \frac{\hat{W}_{-j-1, j} \hat{W}_{-j-2, j+1}}{\hat{W}_{-j-2, -j-1} \hat{W}_{j, j+1}}(\zeta, u_a), \\ \hat{Y}(\zeta, u_a) &= \frac{\hat{W}_{0, r+2}}{\hat{W}_{-1, 0}}(e^{-\frac{i\pi}{2}(r+2)}\zeta, u_a). \end{aligned} \quad (42)$$

Now the Y-system (33) can be written as

$$\begin{aligned} Y_s(e^{\frac{\pi i}{2}}\zeta, u_a) Y_s(e^{-\frac{\pi i}{2}}\zeta, u_a) &= \left(1 + Y_{s-1}(\zeta, u_a)\right) \left(1 + Y_{s+2}(\zeta, u_a)\right), \quad s = 1, \dots, r, \\ Y_{r+1}(e^{\frac{\pi i}{2}}\zeta, u_a) Y_{r+1}(e^{-\frac{\pi i}{2}}\zeta, u_a) &= \left(1 + Y_r(\zeta, u_a)\right) \left(1 + \omega^{\frac{r+3}{2}} e^{2\pi i l} \hat{Y}(\zeta, u_a)\right) \left(1 + \omega^{\frac{r+3}{2}} e^{-2\pi i l} \hat{Y}(\zeta, u_a)\right), \\ \hat{Y}(e^{\frac{\pi i}{2}}\zeta, u_a) \hat{Y}(e^{-\frac{\pi i}{2}}\zeta, u_a) &= 1 + Y_{r+1}(\zeta, u_a), \end{aligned} \quad (43)$$

where $Y_0(\zeta, u_a) = 0$. Since in this Y-system the Y-functions depend on the same u_a 's, we will omit the argument u_a in the Y-functions.

The Y-system (27) and (43) are essentially the same system, but interpretations of the spectral parameter are different. The Y-system (43) also appears in the study of the integrable structure in the minimal model [45], in the massive ODE/IM correspondence for the modified sinh-Gordon equation [19] and in the study of the minimal surface in AdS_3 corresponding to the form factor [34].²

²See also [24, 35] for examples.

3 TBA system

From the analytical properties and asymptotic behaviors of the Y-functions, one can derive a set of non-linear integral equations satisfied by the Y-functions, which is called the Thermodynamic Bethe Ansatz (TBA) equations [46, 47]. Our TBA system turns out to be a massless version of these TBA equations. Similar massive TBA equations can be obtained from the Hitchin system in the study of AdS₃ minimal surface and form factors [31, 34].

3.1 TBA equations

To derive the TBA equations from the Y-system (43), we first need to investigate the small ζ behavior of the Y-functions. The WKB expansion of $\hat{y}_k(x, u_a, \zeta)$ is given by

$$\hat{y}_k(x, u_a, \zeta) = (-1)^{\frac{k}{2}} c(\zeta) \exp\left(\frac{\delta_k}{\zeta} \int_{x_k}^x P(x') dx'\right), \quad (44)$$

where $c(\zeta) = \frac{1}{\sqrt{2i}} \zeta^{\frac{(r+1)}{2(r+3)}}$, and $P(x)$ is expanded in ζ as $P(x, \zeta) = \sum_{n=0}^{\infty} \zeta^n P_n(x)$. From the differential equation (35), $P(x, \zeta)$ satisfies

$$P(x, \zeta)^2 + \delta_k \zeta P'(x, \zeta) - V(x) = 0. \quad (45)$$

We find that $P_0(x) = \sqrt{Q_0(x)}$ and $P_n(x)$ ($n \geq 1$) can be determined recursively. In the exponential of (44), $\delta_k = \pm(-1)^k$ denotes the sign factor, where \pm depends on the plus (minus) sheet of the Riemann surface (the WKB curve) defined by

$$y^2 = Q_0(x) = x^{r+1} + \dots + \frac{u_{r+2}}{x}. \quad (46)$$

We evaluate the Wronskian $\hat{W}_{k_1, k_2}(\zeta)$ by using the WKB solution (44). By choosing the initial points of the solution, we can express the Y-function (42) by using a contour integral over a certain 1-cycle on the curve (46). We find that the Y-functions at small ζ behave as

$$\begin{aligned} \log Y_{2k+1}(\zeta) &\sim -\frac{1}{i\zeta} \oint_{\gamma_{2k+1}} P_0(x) dx =: -\frac{m_{2k+1}}{\zeta}, \\ \log Y_{2k}(\zeta) &\sim -\frac{1}{\zeta} \oint_{\gamma_{2k}} P_0(x) dx =: -\frac{m_{2k}}{\zeta}, \\ \log \hat{Y}(\zeta) &\sim \begin{cases} -\frac{1}{\zeta} \oint_{\hat{\gamma}} P_0(x) dx =: -\frac{\hat{m}}{\zeta} & r : \text{even} \\ -\frac{1}{i\zeta} \oint_{\hat{\gamma}} P_0(x) dx =: -\frac{\hat{m}}{\zeta} & r : \text{odd} \end{cases}. \end{aligned} \quad (47)$$

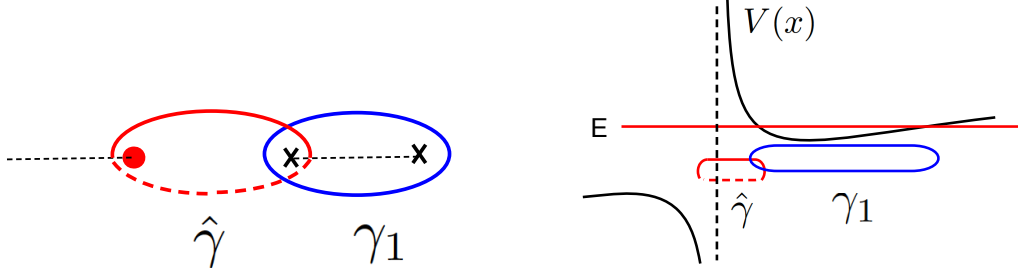


Figure 1: The contour of the Y-functions ($r = 0$) on the Riemann surface $y^2 = \frac{x^2 + u_1 x + u_2}{x}$ is shown on the left. The crosses indicate the turning points satisfying $x^2 + u_1 x + u_2 = 0$. The red dot is the simple pole $x = 0$. The dotted line is the branch cut on the Riemann surface. On the right, we show the corresponding potential and the cycles, where γ_1 and $\hat{\gamma}$ are the classically allowed cycle and classically forbidden cycle respectively.

Note that the above approximation is valid in the sector $|\arg(\zeta)| < \pi$. The classical periods m_s are functions of moduli parameters (u_1, \dots, u_{r+2}) . There are $r + 2$ independent period integrals for m_s for generic u_a 's. γ_s and $\hat{\gamma}$ are the one-cycles on the Riemann surface (46), which possess $r + 2$ turning points and one simple pole. We will consider the case such that all the masses m_s are positive and real.

We choose one-cycles γ_s and $\hat{\gamma}$ on the curve (46) as follows. We show examples of the contours for the $r = 0$ and $r = 1$ case in Fig. 1 and Fig. 2. For $r = 0$, the crossed points indicate the roots of $x^2 + u_1 x + u_2$, which are assumed to be real and positive. The cycle γ_1 encircle the cut between these turning points. While the cycle $\hat{\gamma}$ encircles the simple pole $x = 0$ and one of the root. For $r = 1$ the contours are given as in the $r = 0$ case.

We then introduce the functions $\ell_s(\zeta)$ and $\hat{\ell}(\zeta)$ of ζ , which is analytic in $|\arg(\zeta)| \leq \frac{\pi}{2}$:

$$\ell_s(\zeta) := \log Y_s(\zeta) + \frac{m_s}{\zeta}, \quad \hat{\ell}(\zeta) = \log \hat{Y}(\zeta) + \frac{\hat{m}}{\zeta}. \quad (48)$$

The Y-system then leads to

$$\begin{aligned} \ell_s(e^{\frac{\pi i}{2}} \zeta) + \ell_s(e^{-\frac{\pi i}{2}} \zeta) &= \log \left((1 + Y_{s+1}(\zeta))(1 + Y_{s-1}(\zeta)) \right), \quad s = 1, \dots, r, \\ \ell_{r+1}(e^{\frac{\pi i}{2}} \zeta) + \ell_{r+1}(e^{-\frac{\pi i}{2}} \zeta) &= \log \left((1 + Y_r(\zeta))(1 + \omega^{\frac{r+3}{2}} e^{2\pi i l} \hat{Y}(\zeta))(1 + \omega^{\frac{r+3}{2}} e^{-2\pi i l} \hat{Y}(\zeta)) \right), \\ \hat{\ell}(e^{\frac{\pi i}{2}} \zeta) + \hat{\ell}(e^{-\frac{\pi i}{2}} \zeta) &= \log \left(1 + Y_{r+1}(\zeta, u_a) \right). \end{aligned} \quad (49)$$

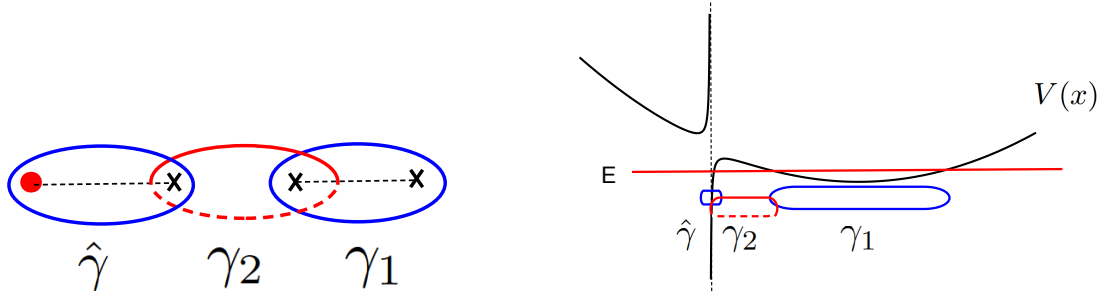


Figure 2: The contours of the Y-function ($r = 1$) on the Riemann surface $y^2 = \frac{x^3+u_1x^2+u_2x+u_3}{x}$ are shown on the left. The crosses indicate the turning points satisfying $x^3 + u_1x^2 + u_2x + u_3 = 0$. The red dot is the simple pole $x = 0$. The dotted line is the branch cut on the Riemann surface. On the right, we show the corresponding potential and the cycles, γ_1 and $\hat{\gamma}$ are the classically allowed cycles, and γ_2 classically forbidden cycle.

Here we set $\zeta = e^{-\theta}$ and introduce the kernel

$$K(\theta) = \frac{1}{2\pi \cosh(\theta)}. \quad (50)$$

Convoluting (49) with the kernel $K(\theta' - \theta)$ on the real axis, the l.h.s picks a pole at $\theta' = \theta$.

One derives the TBA equations

$$\begin{aligned} \log Y_s(\theta) &= -m_s e^\theta + \int_{\mathbb{R}} \frac{\log(1 + Y_{s-1}(\theta')) + \log(1 + Y_{s+1}(\theta'))}{\cosh(\theta - \theta')} \frac{d\theta'}{2\pi}, \quad s = 1, \dots, r, \\ \log Y_{r+1}(\theta) &= -m_{r+1} e^\theta + \int_{\mathbb{R}} \frac{\log(1 + Y_r(\theta'))}{\cosh(\theta - \theta')} \frac{d\theta'}{2\pi} + \int_{\mathbb{R}} \frac{\log\left(\left(1 + \omega^{\frac{r+3}{2}} e^{2\pi i l} \hat{Y}(\theta')\right)\left(1 + \omega^{\frac{r+3}{2}} e^{-2\pi i l} \hat{Y}(\theta')\right)\right)}{\cosh(\theta - \theta')} \frac{d\theta'}{2\pi}, \\ \log \hat{Y}(\theta) &= -\hat{m} e^\theta + \int_{\mathbb{R}} \frac{\log(1 + Y_{r+1}(\theta'))}{\cosh(\theta - \theta')} \frac{d\theta'}{2\pi}. \end{aligned} \quad (51)$$

This TBA system corresponds to the D_{r+3} -type Dynkin diagram Fig.3.

The TBA system (51) can be regarded as the “conformal limit” of the TBA system considered in [34] but with a specific monodromy. Note that in the above derivation, we have assumed that all the masses m_s and \hat{m} to be positive and real. We will explain the TBA equations with complex masses at the end of this section.

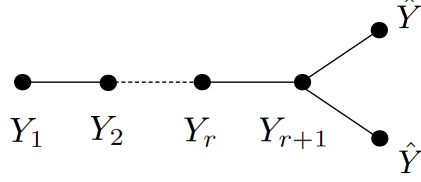


Figure 3: The Dynkin diagram for D_{r+3} -type TBA system.

3.2 Large θ behavior of Y-function

At large θ , the TBA equations (51) lead to the expansion of Y-functions:

$$\begin{aligned}
 -\log Y_s(\theta) &= m_s e^\theta + \sum_{n \geq 1} m_s^{(n)} e^{(1-2n)\theta}, \quad s = 1, \dots, r+1, \\
 -\log \hat{Y}(\theta) &= \hat{m} e^\theta + \sum_{n \geq 1} \hat{m}^{(n)} e^{(1-2n)\theta},
 \end{aligned} \tag{52}$$

where

$$\begin{aligned}
 m_s^{(n)} &= \frac{(-1)^n}{\pi} \int_{\mathbb{R}} e^{(2n-1)\theta} \left\{ \log \left(1 + Y_{s-1}(\theta') \right) + \log \left(1 + Y_{s+1}(\theta') \right) \right\} d\theta', \quad s = 1, \dots, r, \\
 m_{r+1}^{(n)} &= \frac{(-1)^n}{\pi} \int_{\mathbb{R}} e^{(2n-1)\theta} \left\{ \log \left(1 + Y_r(\theta') \right) + \log \left(1 + \omega^{\frac{r+3}{2}} e^{2\pi i l} \hat{Y}(\theta') \right) + \log \left(1 + \omega^{\frac{r+3}{2}} e^{-2\pi i l} \hat{Y}(\theta') \right) \right\} d\theta', \\
 \hat{m}^{(n)} &= \frac{(-1)^n}{\pi} \int_{\mathbb{R}} e^{(2n-1)\theta} \log \left(1 + Y_{r+1}(\theta') \right) d\theta'.
 \end{aligned} \tag{53}$$

By solving the TBA equations (51) numerically, one obtains $m_s^{(n)}$ ($s = 1, \dots, r+1$) and $\hat{m}^{(n)}$. In this way, we can extract the perturbative series of Y-function from the TBA equations. In the next section, we will compare the expansion of Y-functions with the expansion of the WKB periods.

3.3 Effective central charge and “massless” TBA

We can also take the UV limit $\theta \rightarrow -\infty$. As $\theta \rightarrow -\infty$, the Y-function approaches to a constant value $Y_s \rightarrow Y_s^*$, $\hat{Y} \rightarrow \hat{Y}^*$, where

$$Y_s^* = \frac{\sin\left(\frac{\pi(2l+1)}{(r+3)}(s+2)\right) \sin\left(\frac{\pi(2l+1)}{(r+3)}s\right)}{\sin^2\left(\frac{\pi(2l+1)}{(r+3)}\right)}, \quad \hat{Y}^* = \frac{\sin\left(\frac{\pi(2l+1)(r+2)}{(r+3)}\right)}{\sin\left(\frac{\pi(2l+1)}{(r+3)}\right)}. \tag{54}$$

The ‘‘effective central charge’’ associated to our TBA system is defined by

$$c_{\text{eff}} = \frac{6}{\pi^2} \sum_{s=1}^{r+1} m_s \int e^\theta \log(1 + Y_s(\theta)) d\theta + \frac{6}{\pi^2} \hat{m} \int e^\theta \log\left(\left(1 + \omega^{\frac{r+3}{2}} e^{2\pi i l} \hat{Y}(\theta)\right) \left(1 + \omega^{\frac{r+3}{2}} e^{-2\pi i l} \hat{Y}(\theta)\right)\right). \quad (55)$$

In the UV limit, it can be evaluated as

$$c_{\text{eff}} = \frac{6}{\pi^2} \left(\sum_{s=1}^{r+1} \mathcal{L}_1\left(\frac{1}{1 + \frac{1}{Y_s^*}}\right) + \mathcal{L}_{-e^{2\pi i l}}\left(\frac{1}{-e^{2\pi i l} + \frac{1}{\hat{Y}^*}}\right) + \mathcal{L}_{-e^{-2\pi i l}}\left(\frac{1}{-e^{-2\pi i l} + \frac{1}{\hat{Y}^*}}\right) \right), \quad (56)$$

where

$$\mathcal{L}_c(x) = -\frac{1}{2} \int_0^x dy \left(\frac{c \log y}{1 - cy} + \frac{\log(1 - cy)}{y} \right) = \frac{1}{2} \left(\log x \log(1 - cx) + 2\text{Li}_2(cx) \right). \quad (57)$$

and $\text{Li}_2(x)$ is the dilogarithm function. From the dilogarithm identities [48] we find the effective central charge is

$$c_{\text{eff}}(r) = (r + 2) \left(1 - 24 \frac{(l + \frac{1}{2})^2}{r + 3} \right). \quad (58)$$

It is interesting to consider the limit $u_{r+1} \rightarrow 0$ of the TBA equations, where the particle corresponding to \hat{Y} becomes massless, *i.e.* $\hat{m} = 0$. We may label this TBA equations by using the Dynkin diagram in Fig.4. In this case, the constant solution of \hat{Y}

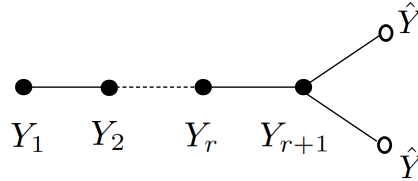


Figure 4: The Dynkin diagram for D_{r+3} -type TBA system with massless \hat{Y} .

will also contribute to the UV limit of the effective central charge of the integrable model. Subtracting this contribution, we thus obtain the effective central charge

$$\begin{aligned} c_{\text{eff}}(r) \Big|_{u_{r+2}=0} &= c_{\text{eff}, D_{r+3}} - c_{\text{eff}, D_2} = c_{\text{eff}}(r) - c_{\text{eff}}(-1) \\ &= r + 1 - 12 \frac{r + 1}{r + 3} \left(l + \frac{1}{2} \right)^2. \end{aligned} \quad (59)$$

Taking the limit $l \rightarrow 0$, we obtain

$$\lim_{l \rightarrow 0} c_{\text{eff}}(r) \Big|_{u_{r+2}=0} = r + 1 - 3 \frac{r + 1}{r + 3} = \frac{r(r + 1)}{r + 3}, \quad (60)$$

which coincides with the one obtained in [39]. When $r = 0$ and $l \neq 0$, the Schrödinger equation (1) recovers the one studied in [8, 9] and [10] for the potential $z + \frac{l(l+1)}{z^2}$. In this case the potential is

$$\lim_{l \rightarrow 0} c_{\text{eff}}(r=0) \Big|_{u_{r+2}=0} = 1 - 4\left(l + \frac{1}{2}\right)^2, \quad (61)$$

which reproduces the effective central charge (D.60) in [10] with $M = 1/2$. We note that when the TBA system has extra discrete symmetry at some points in the moduli space, the central charge must be divided by the discrete symmetry.

3.4 TBA equations for complex mass in minimal chamber

The derivation we presented in section 3.1 is valid for the case with positive and real masses. We now extend the TBA equations (51) to complex masses by following the procedure in [31]. Let us denote the masses by

$$m_s = |m_s|e^{i\phi_s}, \quad \hat{m} = |\hat{m}|e^{i\hat{\phi}}, \quad s = 1, \dots, r+1. \quad (62)$$

We then shift the argument of the Y-function, such that the masses of the shifted Y-functions $Y_s(\theta - i\phi_1)$ and $\hat{Y}(\theta - i\hat{\phi})$ are positive and real. Therefore we obtain the TBA equations:

$$\begin{aligned} \log Y_s(\theta - i\phi_1) &= -|m_s|e^\theta + \int_{\mathbb{R}} \frac{\log\left(1 + Y_{s-1}(\theta' - i\phi_{s-1})\right)}{\cosh(\theta - \theta' - i\phi_s + i\phi_{s-1})} \frac{d\theta'}{2\pi} \\ &\quad + \int_{\mathbb{R}} \frac{\log\left(1 + Y_{s+1}(\theta' - i\phi_{s+1})\right)}{\cosh(\theta - \theta' - i\phi_s + i\phi_{s+1})} \frac{d\theta'}{2\pi}, \quad s = 1, \dots, r, \\ \log Y_{r+1}(\theta - i\phi_{r+1}) &= -|m_{r+1}|e^\theta + \int_{\mathbb{R}} \frac{\log\left(1 + Y_r(\theta' - i\phi_r)\right)}{\cosh(\theta - \theta' - i\phi_{r+1} + i\phi_r)} \frac{d\theta'}{2\pi} \\ &\quad + \int_{\mathbb{R}} \frac{\log\left(1 + \omega^{\frac{r+3}{2}} e^{2\pi i l} \hat{Y}(\theta' - i\hat{\phi})\right)}{\cosh(\theta - \theta' - i\phi_{r+1} + i\hat{\phi})} \frac{d\theta'}{2\pi} + \int_{\mathbb{R}} \frac{\log\left(1 + \omega^{\frac{r+3}{2}} e^{-2\pi i l} \hat{Y}(\theta' - i\hat{\phi})\right)}{\cosh(\theta - \theta' - i\phi_{r+1} + i\hat{\phi})} \frac{d\theta'}{2\pi}, \\ \log \hat{Y}(\theta - i\hat{\phi}) &= -|\hat{m}|e^\theta + \int_{\mathbb{R}} \frac{\log\left(1 + Y_{r+1}(\theta' - i\phi_{r+1})\right)}{\cosh(\theta - \theta' - i\hat{\phi} + i\phi_{r+1})} \frac{d\theta'}{2\pi}. \end{aligned} \quad (63)$$

Note that poles appear in the kernel of these TBA equations when the phases satisfy the conditions:

$$|\phi_s - \phi_{s\pm 1}| = \frac{\pi}{2} \quad \text{or} \quad |\phi_{r+1} - \hat{\phi}| = \frac{\pi}{2}. \quad (64)$$

Hence the TBA equations (63) are valid in the region

$$|\phi_s - \phi_{s\pm 1}| < \frac{\pi}{2} \quad \text{and} \quad |\phi_{r+1} - \hat{\phi}| < \frac{\pi}{2}. \quad (65)$$

This region is called the “minimal chamber” in the moduli space, whose boundary defines the marginal stability wall [27, 28]. In Fig. 5, we plot the curve of marginal stability for the case $Q_0(x) = \frac{x^2 - x + u_2}{x}$, in the complex u_2 plane. The region inside of the wall is the “minimal chamber” for $r = 0$ case.

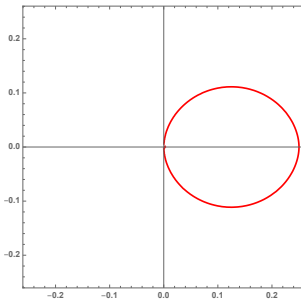


Figure 5: The wall of marginal stability for the case $Q_0(x) = \frac{x^2 - x + u_2}{x}$, in the complex u_2 plane.

As $\phi_s - \phi_{s\pm 1}$ or $\phi_{r+1} - \hat{\phi}$ take the values $\pm \frac{\pi}{2}$, $\pm \frac{3\pi}{2}$, we should modify the form of the TBA equations to include the contribution of the poles (64) in the kernel, where we need to consider the wall-crossing of the TBA equations. More details on the wall crossing will be presented in the appendix B.

4 TBA equations and WKB periods

In the previous work [39], we checked numerically that the WKB periods agree with the large θ -expansion of the logarithm of the Y-function for polynomial potential. In this subsection we confirm this relation for the potential with a regular singularity. The WKB periods $\Pi_\gamma(\zeta)$ for the Schrödinger equation (35) are defined by the period integral

of $P(x, \zeta)$, which are formal even power series of ζ :

$$\Pi_\gamma(\zeta) = \sum_{n \geq 0} \Pi_\gamma^{(n)} \zeta^{2n}, \quad \gamma = \gamma_s, \hat{\gamma}, \quad s = 1, \dots, r+1. \quad (66)$$

The classical periods $\Pi_{\gamma_s}^{(0)}$ and $\Pi_{\hat{\gamma}}^{(0)}$ are determined m_s and \hat{m} respectively using the formulas (47). The ζ^2 correction $\Pi_\gamma^{(1)}$ and the ζ^4 correction $\Pi_\gamma^{(2)}$ of the WKB period are given by

$$\Pi_\gamma^{(1)} = \oint_\gamma dx \left(\frac{1}{2} \frac{Q_2}{\sqrt{Q_0}} + \frac{1}{48} \frac{\partial_x^2 Q_0}{Q_0(x)^{3/2}} \right) \quad (67)$$

and

$$\Pi_\gamma^{(2)} = \oint_\gamma dx \left(-\frac{7}{1536} \frac{(\partial_x^2 Q_0)^2}{Q_0^{7/2}} + \frac{1}{768} \frac{\partial_x^4 Q_0}{Q_0^{5/2}} - \frac{Q_2 \partial_x^2 Q_0}{32 Q_0^{5/2}} + \frac{\partial_x^2 Q_2}{48 Q_0^{3/2}} - \frac{Q_2^2}{8 Q_0^{3/2}} \right) \quad (68)$$

respectively [49]. These higher-order corrections to the WKB periods can be obtained by acting the differential operator on the classical periods. In the present case, following [49–51], we find the formulas

$$\Pi_\gamma^{(1)} = -\frac{1}{12} \sum_{k=0}^{r+1} u_k (r+2-k)(r-k-3) \partial_{u_{k+1}} \partial_{u_{r+2}} \Pi_\gamma^{(0)} + \frac{l(l+1)}{u_{r+2}} \sum_{k=0}^{r+1} u_k (r+1-k) \partial_{u_{k+1}} \Pi_\gamma^{(0)}, \quad (69)$$

$$\begin{aligned} \Pi_\gamma^{(2)} = & \frac{7}{1440} \left[\sum_{i,j=0}^{r-1} [r+1-i]_2 [r+1-j]_2 u_i u_j \partial_{u_{i+1}} \partial_{u_{j+1}} \partial_{u_{r+2}}^2 \right. \\ & + 4u_{r+2} \sum_{i=0}^r u_i \left\{ [r+1-i]_2 - \frac{1}{3}(5r-5i+13) \right\} \partial_{u_{i+2}} \partial_{u_{r+2}}^3 \\ & + \frac{32u_{r+1}}{3} \sum_{k=0}^{r+1} (5r-5k+11) u_k \partial_{u_{k+1}} \partial_{u_{r+2}}^3 \left. \right] \Pi_\gamma^{(0)} \\ & + \frac{1}{768} \left[\frac{8}{3} \sum_{i=0}^{r-3} [r+1-i]_4 u_i \partial_{u_{i+2}} \partial_{u_{r+2}}^2 - 64 \sum_{k=0}^r (r-k+3) u_k \partial_{u_{k+2}} \partial_{u_{r+2}}^2 \right. \\ & + \frac{128u_{r+1}}{u_{r+2}} \sum_{k=0}^{r+1} (3r-3k+7) u_k \partial_{u_{k+1}} \partial_{u_{r+2}}^2 \left. \right] \Pi_\gamma^{(0)} \\ & - \frac{l(l+1)}{12} \left\{ \sum_{k=0}^r u_k (r+2-k)(r-k-3) \partial_{u_{k+2}} + \frac{4u_{r+1}}{u_{r+2}} \sum_{k=0}^{r+1} (3r-3k+7) u_k \partial_{u_{k+1}} \right\} \partial_{u_{r+2}}^2 \Pi_\gamma^{(0)} \\ & - \frac{l(l+1)\{1-l(l+1)\}}{6u_{r+2}} \left\{ \frac{4u_{r+1}}{u_{r+2}} \sum_{k=0}^{r+1} u_k (r-k+3) \partial_{u_{k+1}} - \sum_{k=0}^r u_k (r-k+5) \partial_{u_{k+2}} \right\} \partial_{u_{r+2}} \Pi_\gamma^{(0)}, \quad (70) \end{aligned}$$

where $[a]_k \equiv a(a-1)\cdots(a-k+1)$ and $u_0 = 1$.

4.1 TBA equations and the discontinuity formula

Since the WKB series (66) is an asymptotic expansion in ζ , we define the Borel summation

$$\hat{\Pi}_\gamma(\xi) = \sum_{n \geq 0} \frac{1}{(2n)!} \Pi_\gamma^{(n)} \xi^{2n} \quad (71)$$

and the Borel resummation along the direction φ

$$s_\varphi(\Pi_\gamma)(\hbar) = \frac{1}{\hbar} \int_0^{\infty e^{i\varphi}} e^{-\xi/\hbar} \hat{\Pi}_\gamma(\xi) d\xi. \quad (72)$$

In particular $s(\Pi_\gamma)(\hbar) := s_{\varphi=0}(\Pi_\gamma)(\hbar)$ for $\hbar > 0$ is the usual Borel resummation. Here we use the standard notation: $\hbar := \zeta$. When the resummed period $s(\Pi_\gamma)(\hbar)$ converges for small \hbar , the WKB period Π_γ is said to be Borel summable. When singularities for $\hat{\Pi}_\gamma(\xi)$ exist along a direction φ in the ξ -plane, there arises a discontinuity for $s_\varphi(\Pi_\gamma)(\hbar)$, which is defined by

$$\text{disc}_\varphi \Pi_\gamma(\hbar) = \lim_{\delta \rightarrow 0^+} \left(s(\Pi_\gamma)(e^{i\varphi+i\delta}\hbar) - s(\Pi_\gamma)(e^{i\varphi-i\delta}\hbar) \right). \quad (73)$$

The Delabaere-Pham formula states that the period corresponding to the classically allowed region is not Borel summable along the $\varphi = 0$ direction, while the period for the classically forbidden region being Borel summable [6]. For the WKB period connecting the simple turning points, the discontinuity formula for classically allowed period is given by [6, 43]

$$\frac{i}{\hbar} \text{disc}_{\varphi=0}(\Pi_{\gamma, \text{allowed}})(\hbar) = \log \prod_k \left(1 + \exp \left(-\frac{1}{\hbar} \Pi_{\gamma_k}(\hbar) \right) \right)^{\langle \gamma_k, \gamma \rangle}, \quad (74)$$

where γ_k is the classically forbidden period, $\langle \gamma_k, \gamma \rangle$ is the intersection of the cycles. When the WKB lines connect a turning point and a simple pole, the discontinuity formula has been obtained in [43]. For example, let us consider the period γ' intersecting with $\hat{\gamma}$, such as the γ_1 in Fig.1. When this period is classically allowed, the discontinuity formula reads [43]:

$$\begin{aligned} \frac{i}{\hbar} \text{disc}_{\varphi=0}(\Pi_{\gamma', \text{allowed}})(\hbar) &= \log \prod_k \left(1 + \exp \left(-\frac{1}{\hbar} \Pi_{\gamma_k}(\hbar) \right) \right)^{\langle \gamma_k, \gamma' \rangle} \\ &\quad + \log \left(1 - (e^{2\pi i l} + e^{-2\pi i l}) \exp \left(-\frac{1}{\hbar} \Pi_{\hat{\gamma}}(\hbar) \right) + \exp \left(-2\frac{1}{\hbar} \Pi_{\hat{\gamma}}(\hbar) \right) \right)^{\langle \hat{\gamma}, \gamma' \rangle}. \end{aligned} \quad (75)$$

Moreover, when we rotate $\hbar \rightarrow \pm i\hbar$ for real \hbar , classically allowed and classically forbidden periods are interchanged, which leads to similar discontinuity formulas for other periods.

Let us go back to our case, where $\Pi_{\gamma_{2i+1}}$ and $\Pi_{\gamma_{2i}}$ are classically allowed and classically forbidden respectively. $\Pi_{\hat{\gamma}}$ is classical allowed for odd r , and classically forbidden for even r . We then introduce the functions:

$$\begin{aligned} i \log Y'_{2i+1}(\theta + \frac{\pi i}{2} \pm i\delta) &= \frac{1}{\hbar} s_{\pm\delta}(\Pi_{\gamma_{2i+1}})(\hbar), & -\log Y'_{2i}(\theta) &= \frac{1}{\hbar} \Pi_{2i}(\hbar), \\ \begin{cases} i \log \hat{Y}'(\theta + \frac{\pi i}{2} \pm i\delta) &= \frac{1}{\hbar} s_{\pm\delta}(\Pi_{\hat{\gamma}})(\hbar) & r : \text{odd} \\ -\log \hat{Y}'(\theta) &= \frac{1}{\hbar} \Pi_{\hat{\gamma}}(\hbar) & r : \text{even} \end{cases} \end{aligned} \quad (76)$$

with $\hbar = e^\theta$. In these functions the discontinuity formula take the unified form:

$$\begin{aligned} -\text{disc}_{\frac{\pi}{2}} Y'_s(\theta) &= \log(1 + Y_{s-1}) + \log(1 + Y_{s-1}), & s &= 1, \dots, r, \\ -\text{disc}_{\frac{\pi}{2}} Y'_{r+1}(\theta) &= \log(1 + Y_r(\theta)) + \log(1 - (e^{2\pi i l} + e^{-2\pi i l}) Y_{\hat{\gamma}}(\theta) + Y_{\hat{\gamma}}(\theta)^2), \\ -\text{disc}_{\frac{\pi}{2}} \hat{Y}'(\theta) &= \log(1 + Y_{r+1}(\theta)). \end{aligned} \quad (77)$$

These discontinuity formulas together with the large θ asymptotic behavior of WKB periods, *i.e.*

$$\begin{aligned} -\log Y'_s(\theta) &= m_s e^\theta + \mathcal{O}(e^{-\theta}), & s &= 1, \dots, r+1, \\ -\log \hat{Y}'(\theta) &= \hat{m} e^\theta + \mathcal{O}(e^{-\theta}), & \theta &\rightarrow \infty, \end{aligned} \quad (78)$$

provides the data for the Riemann-Hilbert problem. The solution to this Riemann-Hilbert problem is given by the TBA equations (51), from which we could identify $Y' = Y$. From the relation (76) and comparing the expansion (52) and (66), we find

$$\begin{aligned} m_{2i+1}^{(n)} &= (-1)^n \Pi_{\gamma_{2i+1}}^{(n)}, & m_{2i}^{(n)} &= \Pi_{\gamma_{2i}}^{(n)}, \\ \hat{m}^{(n)} &= \begin{cases} (-1)^n \Pi_{\hat{\gamma}}^{(n)} & r : \text{odd} \\ \Pi_{\hat{\gamma}}^{(n)} & r : \text{even} \end{cases}. \end{aligned} \quad (79)$$

In the following of this section, we will test our TBA equations by comparing $m_a^{(a)}$ and $\hat{m}^{(n)}$ with the higher-order \hbar correction of WKB periods. More precisely, we will focus on the cases with $r = 0$ and $r = 1$.

4.2 $r = 0$ case

Let us consider the case with $r = 0$, where the Schrödinger equation (35) becomes

$$\left(-\hbar^2 \frac{d^2}{dx^2} + \frac{x^2 + u_1 x + u_2}{x} + \hbar^2 \frac{l(l+1)}{x^2} \right) \hat{\psi}(x) = 0. \quad (80)$$

Let e_i ($i = 1, 2$) be the turning points of the potential $Q_0(x)$, i.e. zeros of $x^2 + u_1x + u_2$, which are assumed to be positive real and ordered as

$$0 < e_1 < e_2, \quad (81)$$

$x = 0$ is the pole of the potential. In this case, there are two independent WKB cycles: γ_1 is the cycle connecting e_1 and e_2 , $\hat{\gamma}$ is the cycle connecting 0 and e_1 (Fig.1).

The classical WKB period $\Pi^{(0)}$ can be evaluated explicitly by using the hypergeometric function

$$\Pi_{\gamma_1}^{(0)} = \frac{2}{i} \int_{e_1}^{e_2} \sqrt{\frac{x^2 + u_1x + u_2}{x}} dx = 2 \frac{(e_1 - e_2)^2}{\sqrt{e_1}} \frac{\Gamma(3)}{\Gamma(\frac{1}{2})\Gamma(\frac{3}{2})} F\left(\frac{1}{2}, \frac{3}{2}, 3, \frac{e_1 - e_2}{e_1}\right), \quad (82)$$

$$\Pi_{\hat{\gamma}}^{(0)} = 2 \int_0^{e_1} \sqrt{\frac{x^2 + u_1x + u_2}{x}} dx = 2e_1\sqrt{e_2} \frac{\Gamma(2)}{\Gamma(-\frac{1}{2})\Gamma(\frac{1}{2})} F\left(-\frac{1}{2}, \frac{1}{2}, 2, \frac{e_1}{e_2}\right). \quad (83)$$

Here $F(a, b; c; z)$ is the hypergeometric function whose integral representation is given by³

$$F(a, b; c; x) = \frac{\Gamma(a)\Gamma(b)}{\Gamma(c)} \int_0^1 t^{b-1}(1-t)^{c-b-1}(1-tx)^{-a} dt. \quad (84)$$

The corrections to the classical WKB periods $\Pi_{\gamma}^{(1)}$ and $\Pi_{\gamma}^{(2)}$ can be evaluated by using the formulas (69) and (70) respectively.

On the other hand, we substitute the masses m_1 and \hat{m} given by (47) into the TBA equations, which are given by

$$\begin{aligned} \log Y_1(\theta) &= -m_1 e^\theta + \int_{\mathbb{R}} \frac{\log(1 - \hat{Y}(\theta'))}{\cosh(\theta - \theta')} \frac{d\theta'}{2\pi} + \int_{\mathbb{R}} \frac{\log(1 - \hat{Y}(\theta'))}{\cosh(\theta - \theta')} \frac{d\theta'}{2\pi}, \\ \log \hat{Y}(\theta) &= -\hat{m} e^\theta + \int_{\mathbb{R}} \frac{\log(1 + Y_1(\theta'))}{\cosh(\theta - \theta')} \frac{d\theta'}{2\pi}. \end{aligned} \quad (85)$$

Solving the TBA equations numerically, we evaluate the coefficients (53) of the large θ expansions of the Y-functions.

In Table 1, we compare $m_1^{(n)}$ and $\hat{m}^{(n)}$ ($n = 1, 2$) to the quantum periods $\Pi_{\gamma_1}^{(n)}$ and $\hat{\Pi}^{(n)}$ with fixed u_1, u_2 and l . As we see in this Table, the two calculations agree to the relation (79) in high numeric precision. In the case where $-1 \leq l \leq 0$, i.e. the basis of the solutions $x^{-l} + \dots$ and $x^{-l-1} + \dots$ are regular at $x = 0$, we have tested our TBA equations with high numerical precision.

³We followed the notation of [52], which is different with the notation of ${}_2F_1$ in Mathematica.

n	$\Pi_{\gamma_1}^{(n)}$	$m_1^{(n)}$	$\Pi_{\hat{\gamma}}^{(n)}$	$\hat{m}^{(n)}$
0	3.4222512870	3.4222512870	1.9055241299	1.9055241299
1	0.2960549383	-0.2960549173	-0.1166722969	-0.1166722826
2	0.1580844621	0.1580844602	0.01972364328	0.01972364274

Table 1: The higher-order corrections of the WKB periods for $r = 0$ case with $u_1 = -3$, $u_2 = 1$ and $l = -2/5$. The numerical calculation of the TBA equations is performed by the Fourier discretization with 2^{12} points in the region $(-L, L)$ with the cutoff $L = 25$.

4.2.1 Effective central charge and PNP relation

The formula for the effective central charge (56) can be rewritten in terms of the masses and their next order correction (53):

$$c_{\text{eff}} = -\frac{6}{\pi}(m_1\hat{m}^{(1)} + \hat{m}m_1^{(1)}) = 2\left(1 - 8\left(l + \frac{1}{2}\right)^2\right). \quad (86)$$

This leads to the relations for the quantum periods

$$\Pi_{\gamma_1}^{(0)}\Pi_{\hat{\gamma}}^{(1)} - \Pi_{\hat{\gamma}}^{(0)}\Pi_{\gamma_1}^{(1)} = -\frac{\pi}{3}\left(1 - 8\left(l + \frac{1}{2}\right)^2\right). \quad (87)$$

which is known as the PNP relations or a quantum version of the Matone relations [53–60].

We consider (87) in the limit $u_1 \rightarrow 0$, where the inverse potential term vanishes. In this case, one of the turning points goes to zero. Then the classical period $\Pi_{\hat{\gamma}}^{(0)}$ will vanish. However, the \hbar^2 -order correction $\Pi_{\gamma_1}^{(1)}$ becomes diverge in this limit due to the second term in (69). The l.h.s of (87) remains finite in this limit. We have numerically tested our TBA equations with vanishing \hat{m} against the next order correction of \hat{Y} . We thus found a precise match numerically. Moreover, from the numerical solution, the effective central charge (60) is evaluate as

$$c_{\text{eff}}|_{u_2=0} = 1 - \frac{12\left(l + \frac{1}{2}\right)^2}{3}, \quad (88)$$

which reduces to the one in Appendix D.2 of [10].

4.2.2 Voros spectrum in Bohr-Sommerfeld approximation

Let us now compute the spectrum of Schrödinger equation by using the TBA equations. The discontinuity formula has shown that the classically allowed period Π_{γ_1} is not Borel

summable and need to be resummed for positive and real \hbar . In the context of TBA, the Borel non-summability of Π_{γ_1} means that we will hit a pole after shifting $\theta \rightarrow \theta + \frac{\pi i}{2}$ in $\log Y_1(\theta)$. In this paper, we resumme the period by taking the average of two lateral resummations above and below the singular point, namely ‘‘median’’ resummation denoted by $s_{\text{med}}(\Pi_{\gamma_1})$. In the TBA equations, this resummation can be written as

$$\frac{1}{\hbar} s_{\text{med}}(\Pi_{\gamma_1})(\hbar) = m_1 e^\theta + \text{P} \int_{\mathbb{R}} \frac{\log \left(1 - e^{2\pi i l \hat{Y}(\theta')} \right) \left(1 - e^{-2\pi i l \hat{Y}(\theta')} \right) d\theta'}{\sinh(\theta - \theta')} \frac{d\theta'}{2\pi}, \quad (89)$$

where $\hbar = e^{-\theta}$ and P is the principal value of the singular integral computed by

$$\text{P} \int_{\mathbb{R}} \frac{f(\theta')}{\sinh(\theta - \theta')} d\theta' = \lim_{\delta \rightarrow 0} \int_{\mathbb{R}} \frac{\sinh(\theta - \theta') \cos(\delta)}{\sinh^2(\theta - \theta') \cos^2(\delta) + \cosh^2(\theta - \theta') \sin^2(\delta)} f(\theta') d\theta'. \quad (90)$$

The exact quantization condition for this problem is not known so far. Here, we consider the Bohr-Sommerfeld (BS) quantization condition:

$$\frac{1}{\hbar} s_{\text{med}}(\Pi_{\gamma_1})(\hbar) \sim 2\pi \left(k + \frac{1}{2} \right), \quad k \in \mathbb{Z}_{\geq 0}. \quad (91)$$

In Fig.6, we plot the median resummation of WKB period Π_{γ_1} for $u_1 = -3$, $u_2 = 1$ and

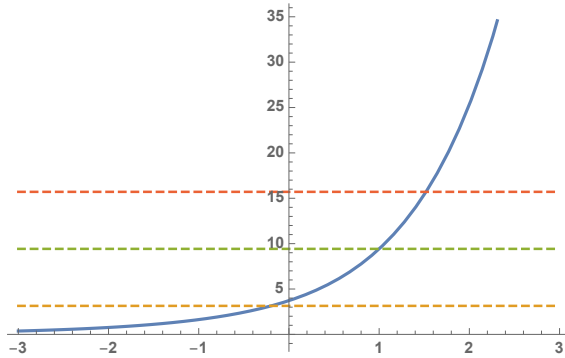


Figure 6: The profile of the median resummation of the WKB period $s_{\text{med}}(\Pi_{\gamma_1})$ as a function of θ for $u_1 = -3$, $u_2 = 1$ and $l = -2/5$. The horizontal dash lines are π , 3π and 5π . We used a discretization with 2^{12} points and the cutoff $L = 50$.

$l = -2/5$, obtaining from the TBA equations. The horizontal dash lines are π , 3π and 5π . The intersect points provide the first three values of Voros spectrum, i.e. the spectrum of $e^{-\theta} = \hbar$ with fixed moduli. In Table 2, we present the Voros spectrum computed from the

Level	$e^{-\theta_{\text{TBA}}}$	$e^{-\theta_{\text{WKB}}}$
0	1.216954845	1.089336418
1	0.367759415	0.363112139
2	0.218798031	0.217867284
3	0.155951604	0.155619488

Table 2: The first column shows the spectrum of values of $e^{-\theta}$ for $u_1 = -3$, $u_2 = 1$ and $l = -2/5$, as computed from the BS quantization condition (91) and the TBA equations (85). The second column shows the spectrum of values of $e^{-\theta}$, as computed from the BS quantization condition (91) and the WKB approximation.

BS quantization condition (91) combined with the TBA equations and the one obtained from the WKB approximation (the BS quantization condition combined with the classical periods). Our numerical result show that the Voros spectrum becomes smaller when level k increases. This means that for large k , where \hbar will be small enough, the driving term $m_1 e^\theta$ in (89) mainly contributes to the periods. Then the WKB approximation becomes valid for higher-level k , which is confirmed by numerical calculations.

4.3 $r = 1$ case

We next consider $r = 1$ case, where the ODE (35) becomes

$$\left(-\hbar^2 \partial_x^2 + \frac{x^3 + u_1 x^2 + u_2 x + u_3}{x} + \hbar^2 \frac{l(l+1)}{x^2} \right) \hat{\psi}(x) = 0. \quad (92)$$

Let us choose the parameters u_1 , u_2 and u_3 such that the zeros e_i ($i = 1, 2, 3$) of $x^3 + u_1 x^2 + u_2 x + u_3$ are positive real and ordered as

$$0 < e_1 < e_2 < e_3. \quad (93)$$

In this case, there are three independent WKB cycles. γ_1 is the cycle connecting e_2 and e_3 . γ_2 is the cycle connecting e_1 and e_2 . $\hat{\gamma}$ is the cycle connecting the pole 0 and e_1 (Fig.2). In this case, all the associated classical WKB periods are positive and real.

Let us now compare the higher-order correction of WKB periods. The u_3 -derivative

of the classical period $\Pi_\gamma^{(0)}$ can be expressed in terms of the hypergeometric function:

$$\begin{aligned}\partial_{u_3}\Pi_{\gamma_1}^{(0)} &= \frac{1}{i} \int_{e_2}^{e_3} dx \frac{1}{\sqrt{x^4 + u_1x^3 + u_2x^2 + u_3x}} \\ &= \frac{1}{i} \frac{1}{\sqrt{e_1e_3 - e_2e_3}} \frac{\Gamma(1)}{\Gamma(\frac{1}{2})\Gamma(\frac{1}{2})} F\left(\frac{1}{2}, \frac{1}{2}; 1; \frac{e_1e_3 - e_1e_2}{e_1e_3 - e_2e_3}\right),\end{aligned}\tag{94}$$

$$\begin{aligned}\partial_{u_3}\Pi_{\gamma_2}^{(0)} &= \int_{e_1}^{e_2} dx \frac{1}{\sqrt{x(x - e_1)(x - e_2)(x - e_3)}} \\ &= \frac{\Gamma(1)}{\Gamma(\frac{1}{2})\Gamma(\frac{1}{2})} \frac{1}{\sqrt{-e_1e_2 + e_2e_3}} F\left(\frac{1}{2}, \frac{1}{2}; 1; \frac{e_1e_3 - e_2e_3}{e_1e_2 - e_2e_3}\right),\end{aligned}\tag{95}$$

$$\begin{aligned}\partial_{u_3}\Pi_{\hat{\gamma}}^{(0)} &= \frac{1}{i} \int_0^{e_1} \frac{1}{\sqrt{x^4 + u_1x^3 + u_2x^2 + u_3x}} dx \\ &= \frac{1}{i} \frac{1}{\sqrt{e_1e_3 - e_2e_3}} \frac{\Gamma(1)}{\Gamma(\frac{1}{2})\Gamma(\frac{1}{2})} F\left(\frac{1}{2}, \frac{1}{2}; 1; \frac{e_1e_3 - e_1e_2}{e_1e_3 - e_2e_3}\right).\end{aligned}\tag{96}$$

From these equations and (69), (70), we can evaluate explicitly $\Pi_\gamma^{(1)}$ and $\Pi_\gamma^{(2)}$.

On the other hand, the TBA system is given by

$$\begin{aligned}\log Y_1(\theta) &= -m_1e^\theta + \int_{\mathbb{R}} \frac{\log(1 + Y_2(\theta'))}{\cosh(\theta - \theta')} \frac{d\theta'}{2\pi}, \\ \log Y_2(\theta) &= -m_1e^\theta + \int_{\mathbb{R}} \frac{\log(1 + Y_1(\theta'))}{\cosh(\theta - \theta')} \frac{d\theta'}{2\pi} + \int_{\mathbb{R}} \frac{\log(1 - e^{2\pi il}\hat{Y}(\theta'))}{\cosh(\theta - \theta')} \frac{d\theta'}{2\pi} \\ &\quad + \int_{\mathbb{R}} \frac{\log(1 - e^{-2\pi il}\hat{Y}(\theta'))}{\cosh(\theta - \theta')} \frac{d\theta'}{2\pi}, \\ \log \hat{Y}(\theta) &= -\hat{m}e^\theta + \int_{\mathbb{R}} \frac{\log(1 + Y_2(\theta'))}{\cosh(\theta - \theta')} \frac{d\theta'}{2\pi}.\end{aligned}\tag{97}$$

where m_1, m_2 and \hat{m} are real and positive. In Table 3, we compare $m_1^{(n)}$ and $\hat{m}_1^{(n)}$, $n = 1, 2$, calculated numerically from (53) by using the TBA equations, to the quantum periods $\Pi_{\gamma_1}^{(n)}$ and $\Pi_{\gamma_2}^{(n)}$ with some fixed values of u_1, u_2, u_3 and l . We find that the two calculations numerically agree with each other and the relation (79) is confirmed. Moreover, eq. (53) predicts that $m_1^{(n)} = \hat{m}^{(n)}$ for all $n > 0$, which is also confirmed for $n = 1, 2$ by numerical calculations. This implies the quantum periods must satisfy $\Pi_{\gamma_1}^{(n)} = \Pi_{\hat{\gamma}}^{(n)}$ for $n > 0$, which is obvious for $n = 1, 2$ because of $\partial_{u_3}\Pi_{\gamma_1}^{(0)} = \partial_{u_3}\Pi_{\hat{\gamma}}^{(0)}$. We have tested our TBA equations with higher numeric precision, when $-1 \leq l \leq 0$, i.e. the basis x^{-l} and x^{-l-1} at $x \rightarrow 0$ are regular.

n	$\Pi_{\gamma_1}^{(n)}$	$m_1^{(n)}$	$\Pi_{\gamma_2}^{(n)}$	$m_2^{(n)}$	$\Pi_{\hat{\gamma}}^{(n)}$	$\hat{m}^{(n)}$
0	6.40730315	6.40730315	0.849415273	0.849415273	4.64015728	4.64015728
1	0.2954268	-0.29542654	0.0602544	0.0602547	0.2954268	-0.29542654
2	0.9636413	0.9636412	-0.009866916	-0.009866912	0.9636413	0.9636412

Table 3: The higher-order corrections of the WKB periods for $r = 1$ case with $u_1 = -13/2$, $u_2 = 10$, $u_3 = -4$ and $l = -1/10$. The numerical calculation of the TBA equations is performed by Fourier discretization with 2^{12} points of the region $(-L, L)$ with the cutoff $L = 25$.

4.3.1 Effective central charge and PNP relation

For $r = 1$, the effective central charge (56) can be rewritten as

$$c_{\text{eff}} = -\frac{6}{\pi}(m_2\hat{m}^{(1)} + \hat{m}m_2^{(1)}) + \frac{6}{\pi^2}(m_1 - \hat{m}) \int_{\mathbb{R}} e^{\theta} \log(1 + Y_1(\theta)) d\theta. \quad (98)$$

In particular, when $m_1 = \hat{m}$ ($\Pi_{\gamma_1}^{(0)} = \Pi_{\hat{\gamma}}^{(0)}$), this leads to the PNP relation:

$$\Pi_{\hat{\gamma}}^{(0)} \Pi_{\gamma_2}^{(1)} - \Pi_{\gamma_2}^{(0)} \Pi_{\hat{\gamma}}^{(1)} = -\frac{\pi}{2} \left(1 - 6\left(l + \frac{1}{2}\right)^2\right). \quad (99)$$

We then consider the case in which $u_3 = 0$, where one of the turning points approaches to zero. The classical period of \hat{Y} will vanish. The numerical solution of effective central charge (60) is evaluate as

$$c_{\text{eff}}|_{u_3=0} = 2 - 6\left(l + \frac{1}{2}\right)^2. \quad (100)$$

Note that taking the limit $l \rightarrow 0$, we obtain the effective central charge $c_{\text{eff}} \rightarrow \frac{1}{2}$, which coincides with the $r = 1$ limit of the effective central charge obtained in [39].

4.3.2 Voros spectrum in Bohr-Sommerfeld approximation

For $r = 1$, the period Π_{γ_1} is non-Borel summable. In the TBA equations, the median resummation of the period is done by

$$\frac{1}{\hbar} s_{\text{med}}(\Pi_{\gamma_1})(\hbar) = m_1 e^{\theta} + \text{P} \int_{\mathbb{R}} \frac{\log(1 + Y_2(\theta'))}{\sinh(\theta - \theta')} \frac{d\theta'}{2\pi}. \quad (101)$$

In Table 4, we calculate the Voros spectrum $e^{-\theta}$ from the TBA equations by using the BS quantization condition and compared them with those of the WKB approximation. The numerical results are similar to the $r = 0$ results.

Level	$e^{-\theta_{\text{TBA}}}$	$e^{-\theta_{\text{WKB}}}$
0	2.110949740	2.039507935
1	0.690146946	0.679835978
2	0.411127634	0.407901587
3	0.292665832	0.291358276

Table 4: The first column shows the spectrum of values of $e^{-\theta}$ for $r = 1$ case with $u_1 = -13/2$, $u_2 = 10$, $u_3 = -4$ and $l = -1/10$, as computed from the BS quantization condition and the TBA equations. The second column shows the spectrum of values of $e^{-\theta}$, as computed from the BS quantization and the WKB approximation.

5 Conclusions and discussions

In this paper, we have derived a set of TBA equations from the Schrödinger equation with polynomial potential and a term with a regular singularity. This provides further non-trivial examples for the ODE/IM correspondence. The TBA equations provide solutions for the Riemann-Hilbert problem of the WKB periods, and govern the exact \hbar -dependence of the WKB periods. From the TBA equations, We have introduced the effective central charge, which coincides the one defined in [39] by taking the limit $l \rightarrow 0$ and $u_{r+2} \rightarrow 0$. The effective central charge also leads to non-trivial constraints on the classical WKB periods and the first-order correction of the WKB periods, which constrains are related to the PNP relations. As an application, we compute numerically the Voros spectrum using the Bohr-Sommerfeld quantization condition.

There are many open questions. In the present paper, we have assumed all the turning points take different values. It is interesting to consider the Schrödinger equations with degenerate potential such as $(x^m - u)^K$, from which one may derive the Hybrid NLIEs in [61–64]. It is also interesting to consider the Schrödinger equation with so-called the monster potential, which corresponds to the excited states of the quantum integral model [65–68]. So far, we have worked out the Schrödinger equation with only one irregular singular point. It is very interesting and important to consider two irregular singular points in the potential, which helps us to study the $\mathcal{N} = 2$ four-dimensional $SU(N)$ super Yang-Mills theory [69–75] and the non-planar scattering amplitude in $\mathcal{N} = 4$ super Yang-Mills theory from the AdS side [76]. The other interesting direction is to study

the higher-order ODEs with polynomial potentials and poles, which are related to the quantum Seiberg-Witten curve of Argyres-Douglas theories in [51, 77].

There are many ODEs are essentially equivalent after the coordinate transformation or parameter redefinitions. One may derive different type TBA equations from these equivalent ODEs. In the appendix C, we have seen these different type TBA equations are essentially equivalent, through a simple but nontrivial example. It is very important to find the general transform rule of the TBA equations under the coordinate transform, which helps us to derive the TBA equations for the ODE with more general potential.

Acknowledgements

We would like to thank Takayasu Kondo, Kohei Kuroda, Marcos Marino, Ryo Suzuki, Roberto Tateo and Dmytro Volin for useful discussions. H.S. would like to thank Jilin University, South China Normal University, Sun Yat-Sen University and Korea Institute for Advanced Study for the warm hospitality. The work of K.I. is supported in part by Grant-in-Aid for Scientific Research 18K03643 and 17H06463 from Japan Society for the Promotion of Science (JSPS). The work of H.S. is supported by the grant ‘‘Exact Results in Gauge and String Theories’’ from the Knut and Alice Wallenberg foundation.

A T-Q relation and Bethe ansatz equation

In this appendix, we derive the T-Q relation from the second order differential equation (1). Let y_k ($k \in \mathbb{Z}$) be a set of solutions obtained by Symanzik rotation. Since (y_0, y_1) form a basis of the solutions, y_k can be expanded as

$$y_k = \frac{W_{k,1}}{W_{0,1}}y_0 + \frac{W_{0,k}}{W_{0,1}}y_1. \quad (102)$$

In particular, y_{-1} is expanded as

$$y_{-1} = \frac{W_{-1,1}}{W_{0,1}}y_0 - \frac{W_{-1,0}}{W_{0,1}}y_1. \quad (103)$$

By using the basis (ψ_+, ψ_-) around $z = 0$ defined in (18), one can expand y_0 in this basis as

$$(2l + 1)y_0 = Q_+\psi_- - Q_-\psi_+, \quad (104)$$

where Q_+ and Q_- are the Q-functions. Taking the Wronskian with y_0 and ψ_{\pm} , we find

$$Q_{\pm}(b_a) = W[y_0, \psi_{\pm}](b_a). \quad (105)$$

By the Symanzik rotation, y_1 is expressed as

$$y_1 = -\omega^{-(l+\frac{1}{2})} \frac{Q_-(\omega^{-a}b_a)}{2l+1} \psi_+ + \omega^{(l+\frac{1}{2})} \frac{Q_+(\omega^{-a}b_a)}{2l+1} \psi_-. \quad (106)$$

From (104) and (106), we obtain

$$\begin{pmatrix} y_1 \\ y_0 \end{pmatrix} (z) = \mathcal{Q}(b_a) \begin{pmatrix} \psi_+ \\ \psi_- \end{pmatrix} (z), \quad \mathcal{Q}(b_a) := \begin{pmatrix} -\omega^{-(l+\frac{1}{2})} \frac{Q_-(\omega^{-a}b_a)}{2l+1} & \omega^{(l+\frac{1}{2})} \frac{Q_+(\omega^{-a}b_a)}{2l+1} \\ -\frac{Q_-(b_a)}{2l+1} & \frac{Q_+(b_a)}{2l+1} \end{pmatrix}. \quad (107)$$

From the Symanzik rotation, we also find

$$\begin{aligned} W[y_k, \psi_+](b_a) &= \omega^{k(l+\frac{1}{2})} W[y, \psi_+](\omega^{-ak}b_a), \\ W[y_k, \psi_-](b_a) &= \omega^{-k(l+\frac{1}{2})} W[y, \psi_-](\omega^{-ak}b_a). \end{aligned} \quad (108)$$

Let us take the Wronskian of y_{-1} in (103) with $\psi_{\pm}(b_a)$. The result is

$$W[y_{-1}, \psi_{\pm}] = \frac{W_{-1,1}}{W_{0,1}} W[y_0, \psi_{\pm}] - \frac{W_{-1,0}}{W_{0,1}} W[y_1, \psi_{\pm}]. \quad (109)$$

Using (105) and (108), we obtain the T-Q relation

$$\frac{W_{-1,1}}{W_{0,1}} Q_{\pm}(b_a) = \omega^{\mp(l+\frac{1}{2})} Q_{\pm}(\omega^a b_a) + \frac{W_{-1,0}}{W_{0,1}} \omega^{\pm(l+\frac{1}{2})} Q_{\pm}(\omega^{-a} b_a), \quad (110)$$

where $\frac{W_{-1,1}}{W_{0,1}}$ is regarded as the T-function. If we set the zeros of Q_a as $b_{a,k}$ ($k \in \mathbb{Z}$):

$$Q_+(b_{a,k}) = 0, \quad (111)$$

then (110) becomes

$$\frac{Q_+(\omega^a b_{a,k})}{Q_+(\omega^{-a} b_{a,k})} = -\frac{W_{-1,0}}{W_{0,1}} \omega^{2(l+\frac{1}{2})}. \quad (112)$$

In our normalization (10), we obtain the Bethe ansatz equation of the form:

$$\frac{Q_+(\omega^a b_{a,k})}{Q_+(\omega^{-a} b_{a,k})} = \begin{cases} -\omega^{2(l+\frac{1}{2})} & r+1 : \text{odd} \\ -\omega^{-2B_{r+\frac{3}{2}}} \omega^{2(l+\frac{1}{2})} & r+1 : \text{even} \end{cases}. \quad (113)$$

B Wall crossing of TBA equations

In section 4, we note that the TBA equations (63) are valid in the minimal chamber (65) in the moduli space. In this appendix, we explain how to analytically continue the TBA equations (63) to outside of the minimal chamber [31, 37, 38]. Here we consider two particular cases: 1) $\frac{\pi}{2} < \phi_2 - \phi_1 < \pi$ while all other difference of phases ϕ are in between $-\pi/2$ and $\pi/2$, 2) $\frac{\pi}{2} < \phi_{r+1} - \hat{\phi} < \pi$ while all other difference of phases ϕ are in between $-\pi/2$ and $\pi/2$. Any other examples of the wall crossing can be treated similarly.

B.1 Case 1: $\phi_2 - \phi_1$ crosses $\pi/2$

When the differences of the phases $\phi_2 - \phi_1$ crosses the value of $\frac{\pi}{2}$ while all other differences of the phases ϕ_s 's and $\hat{\phi}$ are in between $-\pi/2$ and $\pi/2$, we need to modify the integration contour in the TBA equations which results in including the contribution of the pole in the kernel. The TBA system is then modified as

$$\begin{aligned}
 \log Y_1(\theta - i\phi_1) &= -|m_1|e^\theta + \log\left(1 + Y_2(\theta - i\phi_1 - \frac{i\pi}{2} + i\delta)\right) \\
 &\quad + \int_{\mathbb{R}} \frac{\log\left(1 + Y_2(\theta' - i\phi_2)\right)}{\cosh(\theta - \theta' - i\phi_1 + i\phi_2)} \frac{d\theta'}{2\pi} \\
 \log Y_2(\theta - i\phi_2) &= -|m_2|e^\theta + \log\left(1 + Y_1(\theta - i\phi_2 + \frac{i\pi}{2} - i\delta)\right) \\
 &\quad + \int_{\mathbb{R}} \frac{\log\left(1 + Y_1(\theta' - i\phi_1)\right)}{\cosh(\theta - \theta' - i\phi_2 + i\phi_1)} \frac{d\theta'}{2\pi} + \int_{\mathbb{R}} \frac{\log\left(1 + Y_3(\theta' - i\phi_3)\right)}{\cosh(\theta - \theta' - i\phi_2 + i\phi_3)} \frac{d\theta'}{2\pi}.
 \end{aligned} \tag{114}$$

while other TBA equations in (63) are unchanged. However, the arguments of the Y-functions in the second terms of right hand side are different the ones on the left hand side. To obtain a closed TBA system, we need to add the Y-functions with the argument

being shifted. The additional TBA equations are

$$\begin{aligned}
\log Y_1(\theta - i\phi_2 + \frac{i\pi}{2} - i\delta) &= -|m_1|e^{\theta+i\phi_1-i\phi_2+\frac{i\pi}{2}-i\delta} + \log\left(1 + Y_2(\theta - i\phi_2)\right) \\
&\quad + \int_{\mathbb{R}} \frac{\log\left(1 + Y_2(\theta' - i\phi_2)\right) d\theta'}{\cosh(\theta - \theta' + \frac{i\pi}{2} - i\delta) 2\pi}, \\
\log Y_2(\theta - i\phi_1 - \frac{i\pi}{2} + i\delta) &= -|m_2|e^{\theta+i\phi_2-i\phi_1-\frac{i\pi}{2}+i\delta} + \log\left(1 + Y_1(\theta - i\phi_1 + i\delta)\right) \\
&\quad + \int_{\mathbb{R}} \frac{\log\left(1 + Y_1(\theta' - i\phi_1)\right) d\theta'}{\cosh(\theta - \theta' - \frac{i\pi}{2} + i\delta) 2\pi} + \int_{\mathbb{R}} \frac{\log\left(1 + Y_3(\theta' - i\phi_3)\right) d\theta'}{\cosh(\theta - \theta' - i\phi_1 + i\phi_3 - \frac{i\pi}{2} + i\delta) 2\pi}.
\end{aligned} \tag{115}$$

The TBA equations (114) and (115) together with the TBA equations with $a = 3, \dots, r+1$ in (63) provide a closed TBA system.

One may absorb the extra terms $\log\left(1 + Y_{1,2}(\theta - \phi_{2,1} \pm \frac{\pi}{2})\right)$ on the right hand side of (114) to left hand side, and denote them as new Y-functions. As a result, we will obtain a closed TBA system with $r + 3$ Y-functions. This type of wall-crossing of the TBA equations is similar to that of [31, 39].

B.2 Case 2: $\phi_{r+1} - \hat{\phi}$ crosses $\pi/2$

When the phase $\phi_1 - \hat{\phi}$ crosses the value of $\pi/2$, while all other differences of phases are in $(-\frac{\pi}{2}, \frac{\pi}{2})$, we need to modify the TBA equations to

$$\begin{aligned}
\log Y_{r+1}(\theta - i\phi_1) &= -|m_{r+1}|e^\theta + \int_{\mathbb{R}} \frac{\log\left(1 - 2\cos(2\pi l)\hat{Y}(\theta' - \hat{\phi}) + \hat{Y}(\theta' - \hat{\phi})^2\right) d\theta'}{\cosh(\theta - \theta' - i\phi_{r+1} + i\hat{\phi}) 2\pi} \\
&\quad + \log\left(1 - 2\cos(2\pi l)\hat{Y}(\theta - i\phi_{r+1} + \frac{i\pi}{2}) + \hat{Y}(\theta - i\phi_{r+1} + \frac{i\pi}{2})^2\right), \\
\log \hat{Y}(\theta - i\hat{\phi}) &= -|\hat{m}|e^\theta + \int_{\mathbb{R}} \frac{\log\left(1 + Y_{r+1}(\theta' - i\hat{\phi})\right) d\theta'}{\cosh(\theta - \theta' - i\hat{\phi} + i\phi_{r+1}) 2\pi} + \log\left(1 + Y_{r+1}(\theta - i\hat{\phi} - \frac{i\pi}{2})\right).
\end{aligned} \tag{116}$$

Note that $Y_{r+1}(\theta - i\hat{\phi} - \frac{i\pi}{2})$ and $\hat{Y}(\theta - i\phi_{r+1} + \frac{i\pi}{2})$ do not appear on the left hand side. To obtain a closed TBA system, we evaluate the TBA equations at $\theta + i\phi_{r+1} - i\hat{\phi} - \frac{i\pi}{2}$

and $\theta + i\hat{\phi} - i\phi_{r+1} + \frac{i\pi}{2}$, and obtain

$$\begin{aligned}
\log Y_{r+1}\left(\theta - i\hat{\phi} - \frac{i\pi}{2}\right) &= -|m_{r+1}|e^{\theta+i\phi_{r+1}-i\hat{\phi}-\frac{i\pi}{2}} + \int_{\mathbb{R}} \frac{\log\left(1 - 2\cos(2\pi l)\hat{Y}(\theta' - \hat{\phi}) + \hat{Y}(\theta' - \hat{\phi})^2\right)}{\cosh\left(\theta - \theta' - \frac{i\pi}{2}\right)} \frac{d\theta'}{2\pi} \\
&\quad + \log\left(1 - 2\cos(2\pi l)\hat{Y}(\theta - i\hat{\phi}) + \hat{Y}(\theta - i\hat{\phi})^2\right), \\
\log \hat{Y}\left(\theta - i\phi_{r+1} + \frac{i\pi}{2}\right) &= -|\hat{m}|e^{\theta+i\hat{\phi}-i\phi_{r+1}+\frac{i\pi}{2}} + \int_{\mathbb{R}} \frac{\log\left(1 + Y_{r+1}(\theta' - i\phi_{r+1})\right)}{\cosh\left(\theta - \theta' + \frac{i\pi}{2}\right)} \frac{d\theta'}{2\pi} \\
&\quad + \log\left(1 + Y_{r+1}(\theta - i\phi_{r+1})\right).
\end{aligned} \tag{117}$$

These two equations together with (116) and the TBA equations with $s = 1, \dots, r$ in (63) form a closed TBA system.

C Duality between ODEs

In this appendix, we discuss the relations among the present ODE and other types of ODEs under a change of variable $x \rightarrow \tilde{x}$. This relation provides a further consistency check of the correspondence between the ODEs and the TBA systems. The Schrödinger type equation (35) is related with the Schrödinger type equation studied in [39] by coordinate transformation $x \rightarrow \tilde{x}$. Then it is natural to ask how the TBA equations (51) are related with the TBA equations found in [39]. More general, one may consider the transformation from the ODE in x (ODE_x) to the ODE in \tilde{x} ($\widetilde{\text{ODE}}_{\tilde{x}}$), and ask how their TBA equations transform in this procedure. This may help us to find the TBA equations for the ODE with more general potential. In this appendix, we start with certain Schrödinger-type equation with polynomial potential studied in [39] and their TBA equations in the minimal chamber. We then impose the coordinate transformation to get the Schrödinger type equation (35). By comparing their TBA equations, we show how they are related to each other.

Let us begin with the Schrödinger equation with potential of even power polynomial in x , which has been studied in [39]

$$\left(-\zeta^2 \frac{d^2}{dx^2} + x^{2n} + u_1 x^{2(n-1)} + u_2 x^{2(n-2)} + \dots + u_n\right)\psi = 0 \tag{118}$$

with a positive integer $n > 1$. We assume that all the turning points are real and ordered as

$$-a_1 < -a_2 \cdots < -a_n < a_n < \cdots < a_2 < a_1. \quad (119)$$

In this case we obtain the A_{2n-1}/Z_2 -type TBA equations

$$\begin{aligned} \log Y_1(\theta) &= -m_1 e^\theta + \int_{\mathbb{R}} \frac{\log(1 + Y_2(\theta'))}{\cosh(\theta - \theta')} \frac{d\theta'}{2\pi}, \\ \log Y_2(\theta) &= -m_2 e^\theta + \int_{\mathbb{R}} \frac{\log(1 + Y_1(\theta'))}{\cosh(\theta - \theta')} \frac{d\theta'}{2\pi} + \int_{\mathbb{R}} \frac{\log(1 + Y_3(\theta'))}{\cosh(\theta - \theta')} \frac{d\theta'}{2\pi}, \\ &\vdots, \\ \log Y_n(\theta) &= -m_n e^\theta + 2 \int_{\mathbb{R}} \frac{\log(1 + Y_{n-1}(\theta'))}{\cosh(\theta - \theta')} \frac{d\theta'}{2\pi}. \end{aligned} \quad (120)$$

The masses are given by

$$\begin{aligned} m_{2k+1} &= \frac{2}{i} \int_{a_{2k+1}}^{a_{2k+2}} \sqrt{x^{2n} + u_1 x^{2(n-1)} + \cdots + u_n} dx, \\ m_{2k} &= 2 \int_{a_{2k}}^{a_{2k+1}} \sqrt{x^{2n} + u_1 x^{2(n-1)} + \cdots + u_n} dx, \end{aligned} \quad (121)$$

where $1 \leq 2k, 2k+1 \leq n$.

Setting $x^2 = \tilde{x}$, the Schrödinger equation (118) becomes

$$\left(-\zeta^2 \frac{d^2}{d\tilde{x}^2} + \frac{1}{4} \tilde{x}^{n-1} + \frac{u_1}{4} \tilde{x}^{n-2} + \frac{u_2}{4} \tilde{x}^{n-3} + \cdots + \frac{u_n}{4\tilde{x}} - \zeta^2 \frac{3}{16\tilde{x}^2} \right) \tilde{\psi}(\tilde{x}) = 0, \quad (122)$$

where $\tilde{\psi}(\tilde{x}) = e^{-\frac{1}{2} \int \frac{1}{2\tilde{x}} d\tilde{x}} \psi(x)$. Note that this Schrödinger equation has the form of (35) but with $l = -\frac{1}{4}$ or $-\frac{3}{4}$. The turning points are

$$a_n^2 < \cdots < a_2^2 < a_1^2. \quad (123)$$

The TBA equations are

$$\begin{aligned}
\log \tilde{Y}_1(\theta) &= -\tilde{m}_1 e^\theta + \int_{\mathbb{R}} \frac{\log(1 + \tilde{Y}_2(\theta'))}{\cosh(\theta - \theta')} \frac{d\theta'}{2\pi}, \\
\log \tilde{Y}_2(\theta) &= -\tilde{m}_2 e^\theta + \int_{\mathbb{R}} \frac{\log(1 + \tilde{Y}_1(\theta'))}{\cosh(\theta - \theta')} \frac{d\theta'}{2\pi} + \int_{\mathbb{R}} \frac{\log(1 + \tilde{Y}_3(\theta'))}{\cosh(\theta - \theta')} \frac{d\theta'}{2\pi}, \\
&\vdots, \\
\log \tilde{Y}_{n-1}(\theta) &= -\tilde{m}_{n-1} e^\theta + \int_{\mathbb{R}} \frac{\log(1 + \tilde{Y}_{n-2}(\theta'))}{\cosh(\theta - \theta')} \frac{d\theta'}{2\pi} + \int_{\mathbb{R}} \frac{\log(1 + \tilde{Y}(\theta')^2)}{\cosh(\theta - \theta')} \frac{d\theta'}{2\pi}, \\
\log \tilde{Y}(\theta) &= -\tilde{m} e^\theta + \int_{\mathbb{R}} \frac{\log(1 + \tilde{Y}_2(\theta'))}{\cosh(\theta - \theta')} \frac{d\theta'}{2\pi},
\end{aligned} \tag{124}$$

whose masses are given by

$$\begin{aligned}
\tilde{m}_{2k+1} &= \frac{2}{i} \int_{a_{2k+2}^2}^{a_{2k+1}^2} \sqrt{\frac{\tilde{x}^n + u_1 \tilde{x}^{n-1} + u_2 \tilde{x}^{n-2} + \dots + u_n}{4\tilde{x}}} d\tilde{x}, \\
\tilde{m}_{2k} &= 2 \int_{a_{2k+1}^2}^{a_{2k}^2} \sqrt{\frac{\tilde{x}^n + u_1 \tilde{x}^{n-1} + u_2 \tilde{x}^{n-2} + \dots + u_n}{4\tilde{x}}} d\tilde{x}, \quad 1 \leq 2k, 2k+1 \leq n-1, \\
\tilde{m} &= \begin{cases} \frac{2}{i} \int_0^{a_n} \sqrt{(x^{2n} + u_1 x^{2(n-1)} + u_2 x^{2(n-2)} + \dots + u_n)} & n : \text{odd} \\ 2 \int_0^{a_n} \sqrt{(x^{2n} + u_1 x^{2(n-1)} + u_2 x^{2(n-2)} + \dots + u_n)} & n : \text{even} \end{cases}.
\end{aligned} \tag{125}$$

After simple calculations, we find

$$\tilde{m}_a = m_a, \quad \tilde{m} = \frac{1}{2} m_n \quad \text{for } a = 1, \dots, n-1. \tag{126}$$

Comparing with the TBA equations (120) and (124), we find

$$\tilde{Y}_1(\theta) = Y_1(\theta), \quad \tilde{Y}_2(\theta) = Y_2(\theta), \dots, \tilde{Y}_{n-1}(\theta) = Y_{n-1}(\theta), \quad \tilde{Y}(\theta)^2 = Y_n(\theta). \tag{127}$$

Therefore, the two sets of TBA equation derived from (118) and (122) respectively are related with each other by redefinition.

References

- [1] R. Balian, G. Parisi and A. Voros, ‘‘Quartic Oscillator,’’ Lecture Notes in Physics, vol. 106 (1979) 337-360

- [2] A. Voros, “Spectre de l’équation de Schrödinger et méthode BKW”, Publications Mathématiques d’Orsay, France, 1981.
- [3] A. Voros. “The return of the quartic oscillator. The complex WKB method”, Ann. I.H.P. 39 (1983) 211.
- [4] H. Dillinger, E. Delabaere and F. Pham, “Résurgence de voros et périodes des courbes hyperelliptiques”, Annales Inst.Fourier,43 (1993) 163.
- [5] E. Delabaere, H. Dillinger and F. Pham, “Exact semiclassical expansions for one-dimensional quantum oscillators”. J.Math.Phys. 38 (1997) 6126.
- [6] E. Delabaere and F. Pham, “Resurgent methods in semi-classical asymptotics”, Ann. I.H.P. 71 (1999) 1.
- [7] P. Dorey and R. Tateo, “Anharmonic oscillators, the thermodynamic Bethe ansatz, and nonlinear integral equations,” J. Phys. A **32**, L419 (1999) [hep-th/9812211].
- [8] V. V. Bazhanov, S. L. Lukyanov and A. B. Zamolodchikov, “Spectral determinants for Schrodinger equation and Q operators of conformal field theory,” J. Statist. Phys. **102**, 567 (2001) [hep-th/9812247].
- [9] P. Dorey and R. Tateo, “On the relation between Stokes multipliers and the T-Q systems of conformal field theory,” Nucl. Phys. B **563**, 573 (1999) Erratum: [Nucl. Phys. B **603**, 581 (2001)] [hep-th/9906219].
- [10] P. Dorey, C. Dunning and R. Tateo, “The ODE/IM Correspondence,” J. Phys. A **40**, R205 (2007) [hep-th/0703066].
- [11] P. Dorey and R. Tateo, “Differential equations and integrable models: The SU(3) case,” Nucl. Phys. B **571**, 583 (2000) Erratum: [Nucl. Phys. B **603**, 582 (2001)] [hep-th/9910102].
- [12] J. Suzuki, “Functional relations in Stokes multipliers and solvable models related to $U_q(A_n^{(1)})$,” J. Phys. A **33**, 3507 (2000) [hep-th/9910215].

- [13] P. Dorey, C. Dunning and R. Tateo, “Differential equations for general $SU(n)$ Bethe ansatz systems,” *J. Phys. A* **33**, 8427 (2000) [hep-th/0008039].
- [14] J. Suzuki, “Stokes multipliers, spectral determinants and T-Q relations,” *RIMS Kokyuroku* **1221**, 21 (2001) [nlin/0009006 [nlin-si]].
- [15] P. Dorey, C. Dunning, D. Masoero, J. Suzuki and R. Tateo, “Pseudo-differential equations, and the Bethe ansatz for the classical Lie algebras,” *Nucl. Phys. B* **772**, 249 (2007) [hep-th/0612298].
- [16] J. Sun, “Polynomial relations for q -characters via the ODE/IM correspondence,” *SIGMA* **8**, 028 (2012) [arXiv:1201.1614 [math.QA]].
- [17] D. Masoero, A. Raimondo and D. Valeri, “Bethe Ansatz and the Spectral Theory of Affine Lie Algebra-Valued Connections I. The simply-laced Case,” *Commun. Math. Phys.* **344**, no. 3, 719 (2016) [arXiv:1501.07421 [math-ph]].
- [18] D. Masoero, A. Raimondo and D. Valeri, “Bethe Ansatz and the Spectral Theory of Affine Lie algebra-Valued Connections II: The Non Simply-Laced Case,” *Commun. Math. Phys.* **349**, no. 3, 1063 (2017) [arXiv:1511.00895 [math-ph]].
- [19] S. L. Lukyanov and A. B. Zamolodchikov, “Quantum Sine(h)-Gordon Model and Classical Integrable Equations,” *JHEP* **1007**, 008 (2010) [arXiv:1003.5333 [math-ph]].
- [20] P. Dorey, S. Faldella, S. Negro and R. Tateo, “The Bethe Ansatz and the Tzitzeica-Bullough-Dodd equation,” *Phil. Trans. Roy. Soc. Lond. A* **371**, 20120052 (2013) [arXiv:1209.5517 [math-ph]].
- [21] K. Ito and C. Locke, “ODE/IM correspondence and modified affine Toda field equations,” *Nucl. Phys. B* **885**, 600 (2014) [arXiv:1312.6759 [hep-th]].
- [22] P. Adamopoulou and C. Dunning, “Bethe Ansatz equations for the classical $A_n^{(1)}$ affine Toda field theories,” *J. Phys. A* **47**, 205205 (2014) [arXiv:1401.1187 [math-ph]].

- [23] K. Ito and C. Locke, “ODE/IM correspondence and Bethe ansatz for affine Toda field equations,” Nucl. Phys. B **896**, 763 (2015) [arXiv:1502.00906 [hep-th]].
- [24] K. Ito and H. Shu, “ODE/IM correspondence for modified $B_2^{(1)}$ affine Toda field equation,” Nucl. Phys. B **916**, 414 (2017) [arXiv:1605.04668 [hep-th]].
- [25] K. Ito and H. Shu, “Massive ODE/IM Correspondence and Non-linear Integral Equations for $A_r^{(1)}$ -type modified Affine Toda Field Equations,” J. Phys. A **51**, no. 38, 385401 (2018) [arXiv:1805.08062 [hep-th]].
- [26] M. Kontsevich and Y. Soibelman, “Stability structures, motivic Donaldson-Thomas invariants and cluster transformations,” arXiv:0811.2435 [math.AG].
- [27] D. Gaiotto, G. W. Moore and A. Neitzke, “Four-dimensional wall-crossing via three-dimensional field theory,” Commun. Math. Phys. **299**, 163 (2010) [arXiv:0807.4723 [hep-th]].
- [28] D. Gaiotto, G. W. Moore and A. Neitzke, “Wall-crossing, Hitchin Systems, and the WKB Approximation,” arXiv:0907.3987 [hep-th].
- [29] L. F. Alday and J. Maldacena, “Null polygonal Wilson loops and minimal surfaces in Anti-de-Sitter space,” JHEP **0911**, 082 (2009) [arXiv:0904.0663 [hep-th]].
- [30] L. F. Alday, D. Gaiotto and J. Maldacena, “Thermodynamic Bubble Ansatz,” JHEP **1109**, 032 (2011) [arXiv:0911.4708 [hep-th]].
- [31] L. F. Alday, J. Maldacena, A. Sever and P. Vieira, “Y-system for Scattering Amplitudes,” J. Phys. A **43**, 485401 (2010) [arXiv:1002.2459 [hep-th]].
- [32] Y. Hatsuda, K. Ito, K. Sakai and Y. Satoh, “Thermodynamic Bethe Ansatz Equations for Minimal Surfaces in AdS_3 ,” JHEP **1004**, 108 (2010) [arXiv:1002.2941 [hep-th]].
- [33] A. Cavaglia, D. Fioravanti and R. Tateo, “Extended Y-system for the AdS_5/CFT_4 correspondence,” Nucl. Phys. B **843**, 302 (2011) [arXiv:1005.3016 [hep-th]].
- [34] J. Maldacena and A. Zhiboedov, “Form factors at strong coupling via a Y-system,” JHEP **1011**, 104 (2010) [arXiv:1009.1139 [hep-th]].

- [35] Z. Gao and G. Yang, “Y-system for form factors at strong coupling in AdS_5 and with multi-operator insertions in AdS_3 ,” JHEP **1306**, 105 (2013) [arXiv:1303.2668 [hep-th]].
- [36] D. Gaiotto, “Opers and TBA,” arXiv:1403.6137 [hep-th].
- [37] J. Toledo. 2010. Notes on wall-crossing, unpublished.
- [38] J. Toledo. 2016. Exact results in QFT: minimal areas and maximal couplings, Ph.D. thesis, University of Waterloo, Waterloo, ON, Canada.
- [39] K. Ito, M. Mariño and H. Shu, “TBA equations and resurgent Quantum Mechanics,” JHEP **1901**, 228 (2019) [arXiv:1811.04812 [hep-th]].
- [40] J. Suzuki, “Elementary functions in Thermodynamic Bethe Ansatz,” J. Phys. A **48**, no. 20, 205204 (2015) [arXiv:1501.00773 [math-ph]].
- [41] E. Delabaere and J.-M. Rasoamanana, “Resurgent Deformations for an Ordinary Differential Equation of Order 2,” Pacific Journal of Mathematics 223, 1 (2006) [math/0403085].
- [42] K. Iwaki and T. Nakanishi. 2014. “Exact WKB analysis and cluster algebras,” J. Phys. A **47**, 474009 arXiv:1401.7094
- [43] K. Iwaki and T. Nakanishi, “Exact WKB analysis and cluster algebras II: Simple poles, orbifold points, and generalized cluster algebras,” [arXiv:1409.4641].
- [44] Y. Sibuya, Global Theory of a second-order linear ordinary differential operator with polynomial coefficient (Amsterdam: North-Holland 1975)
- [45] V. V. Bazhanov, S. L. Lukyanov and A. B. Zamolodchikov, “Integrable quantum field theories in finite volume: Excited state energies,” Nucl. Phys. B **489**, 487 (1997) [hep-th/9607099].
- [46] C. N. Yang and C. P. Yang, “Thermodynamics of one-dimensional system of bosons with repulsive delta function interaction,” J. Math. Phys. **10**, 1115 (1969).

- [47] A. B. Zamolodchikov, “Thermodynamic Bethe Ansatz in Relativistic Models. Scaling Three State Potts and Lee-yang Models,” Nucl. Phys. B **342**, 695 (1990).
- [48] A. N. Kirillov, “Identities for the Rogers dilogarithm function connected with simple Lie algebras,” Zap. Nauchn. Semin. Leningr. Otdel. Mat. Inst. **164** (1987) 121 [J. Math. Sci. **47** (1989) 2450].
- [49] K. Ito, S. Kanno and T. Okubo, “Quantum periods and prepotential in $\mathcal{N} = 2$ SU(2) SQCD,” JHEP **1708**, 065 (2017) [arXiv:1705.09120 [hep-th]].
- [50] K. Ito and T. Okubo, “Quantum periods for $\mathcal{N} = 2$ SU(2) SQCD around the superconformal point,” Nucl. Phys. B **934**, 356 (2018) [arXiv:1804.04815 [hep-th]].
- [51] K. Ito, S. Koizumi and T. Okubo, “Quantum Seiberg-Witten curve and Universality in Argyres-Douglas theories,” Phys. Lett. B **792**, 29 (2019) [arXiv:1903.00168 [hep-th]].
- [52] T. Masuda and H. Suzuki, “Periods and prepotential of N=2 SU(2) supersymmetric Yang-Mills theory with massive hypermultiplets,” Int. J. Mod. Phys. A **12**, 3413 (1997) [Int. J. Mod. Phys. A **12**, 9700179 (1997)] [hep-th/9609066].
- [53] M. Matone, “Instantons and recursion relations in N=2 SUSY gauge theory,” Phys. Lett. B **357**, 342 (1995) [hep-th/9506102].
- [54] J. Sonnenschein, S. Theisen and S. Yankielowicz, “On the relation between the holomorphic prepotential and the quantum moduli in SUSY gauge theories,” Phys. Lett. B **367**, 145 (1996) [hep-th/9510129].
- [55] T. Eguchi and S. K. Yang, “Prepotentials of N=2 supersymmetric gauge theories and soliton equations,” Mod. Phys. Lett. A **11**, 131 (1996) [hep-th/9510183].
- [56] G. V. Dunne and M. Unsal, “Uniform WKB, Multi-instantons, and Resurgent Trans-Series,” Phys. Rev. D **89**, no. 10, 105009 (2014) [arXiv:1401.5202 [hep-th]].
- [57] A. Gorsky and A. Milekhin, “RG-Whitham dynamics and complex Hamiltonian systems,” Nucl. Phys. B **895**, 33 (2015) [arXiv:1408.0425 [hep-th]].

- [58] G. Basar and G. V. Dunne, “Resurgence and the Nekrasov-Shatashvili limit: connecting weak and strong coupling in the Mathieu and Lamé systems,” *JHEP* **1502**, 160 (2015) [arXiv:1501.05671 [hep-th]].
- [59] S. Codesido and M. Marino, “Holomorphic Anomaly and Quantum Mechanics,” *J. Phys. A* **51**, no. 5, 055402 (2018) [arXiv:1612.07687 [hep-th]].
- [60] G. Basar, G. V. Dunne and M. Unsal, “Quantum Geometry of Resurgent Perturbative/Nonperturbative Relations,” *JHEP* **1705**, 087 (2017) [arXiv:1701.06572 [hep-th]].
- [61] J. Suzuki, “Spinons in magnetic chains of arbitrary spins at finite temperature,” *J. Phys. A* **32**, 2341 (1999).
- [62] J. Suzuki, “Excited states nonlinear integral equations for an integrable anisotropic spin 1 chain,” *J. Phys. A* **37**, 11957 (2004) [hep-th/0410243].
- [63] C. Dunning, “Finite size effects and the supersymmetric sine-Gordon models,” *J. Phys. A* **36**, 5463 (2003) [hep-th/0210225].
- [64] C. Babenko and F. Smirnov, “Suzuki equations and integrals of motion for supersymmetric CFT,” *Nucl. Phys. B* **924**, 406 (2017) [arXiv:1706.03349 [hep-th]].
- [65] V. V. Bazhanov, S. L. Lukyanov and A. B. Zamolodchikov, “Higher level eigenvalues of Q operators and Schroedinger equation,” *Adv. Theor. Math. Phys.* **7**, no. 4, 711 (2003) [hep-th/0307108].
- [66] D. Masoero and A. Raimondo, “Opers for higher states of quantum KdV models,” arXiv:1812.00228 [math-ph].
- [67] V. V. Bazhanov, G. A. Kotousov, S. M. Koval and S. L. Lukyanov, “On the scaling behaviour of the alternating spin chain,” *JHEP* **1908**, 087 (2019) [arXiv:1903.05033 [hep-th]].
- [68] G. A. Kotousov and S. L. Lukyanov, “Bethe state norms for the Heisenberg spin chain in the scaling limit,” arXiv:1906.07081 [hep-th].

- [69] Zamolodchikov, A.B.. 2012. World Scientific. Generalized Mathieu equations and Liouville TBA, in Quantum Field Theories in Two Dimensions, vol. 2.
- [70] A. Grassi and M. Mariño “A Solvable Deformation of Quantum Mechanics,” SIGMA **15**, 025 (2019) [arXiv:1806.01407 [hep-th]].
- [71] K. Ito and H. Shu, “Generalized ODE/IM correspondence and its application to $N=2$ gauge theories”, poster presented at the conference String Math 2018 (2018).
- [72] L. Hollands and A. Neitzke, “Exact WKB and abelianization for the T_3 equation,” arXiv:1906.04271 [hep-th].
- [73] A. Grassi, J. Gu and M. Mariño, “Non-perturbative approaches to the quantum Seiberg-Witten curve,” arXiv:1908.07065 [hep-th].
- [74] D. Fioravanti and D. Gregori, “Integrability and cycles of deformed $\mathcal{N} = 2$ gauge theory,” arXiv:1908.08030 [hep-th].
- [75] D. Fioravanti, H. Poghosyan and R. Poghossian, “ T , Q and periods in $SU(3)$ $\mathcal{N} = 2$ SYM,” arXiv:1909.11100 [hep-th].
- [76] R. Ben-Israel, A. G. Tumanov and A. Sever, “Scattering amplitudes-Wilson loops duality for the first non-planar correction,” JHEP **1808**, 122 (2018) [arXiv:1802.09395 [hep-th]].
- [77] K. Ito and H. Shu, “ODE/IM correspondence and the Argyres-Douglas theory,” JHEP **1708**, 071 (2017) [arXiv:1707.03596 [hep-th]].